~~CONFIDENTIAL~~

Copy 4
RM L58B21

NACA

RESEARCH MEMORANDUM

THEORETICAL ANALYSIS OF THE INTERFERENCE EFFECTS OF SEVERAL SUPERSONIC-TUNNEL WALLS CAPABLE OF ABSORBING THE SHOCK CAUSED BY THE NOSE OF A MODEL

By Clarence W. Matthews

Langley Aeronautical Laboratory
Langley Field, Va.

CLASSIFIED DOCUMENT

NATIONAL ADVISORY COMMITTEE
FOR AERONAUTICS

WASHINGTON

May 26, 1958

~~CONFIDENTIAL~~

NATIONAL ADVISORY COMMITTEE FOR AERONAUTICS

RESEARCH MEMORANDUM

THEORETICAL ANALYSIS OF THE INTERFERENCE EFFECTS OF SEVERAL SUPERSONIC-TUNNEL WALLS CAPABLE OF ABSORBING THE SHOCK CAUSED BY THE NOSE OF A MODEL

By Clarence W. Matthews

SUMMARY

A theoretical analysis was made of the supersonic flow about two-dimensional and three-dimensional axially symmetric models restricted by theoretical walls capable of removing the nose shock. Walls which obeyed a nonreflecting condition were found to be not necessarily non-interfering; severe interference might occur if the wall did not tie the flow to a free-field or free-stream condition. The noninterfering condition was found to be more stringent than the nonreflecting condition and also was found to be practically unattainable in any tunnel. A relation between the pressure difference across the wall and the flow through the wall was used to determine the effects of porous walls. Even though the porous walls removed the effects of the initial shock, they generally produced other rather severe interference effects. A comparison of some theoretical results of this paper with experimental results of a similar study suggested that the thick boundary layer which results from inflow through the wall has a very strong influence on the effective porosity of the tunnel.

INTRODUCTION

Wind-tunnel interference at Mach numbers only a little greater than unity may be both severe and difficult to correct. Such interference is most evident as a reflection of the bow wave striking the test model. The reflected disturbance may be observed by the schlieren method or by measurements of the pressure wave at the surface of the model. Other types of interference not so easily observed are not, however, precluded.

With the minimization or elimination of the subsonic blockage interference by means of partly open and partly closed walls (refs. 1 and 2), the idea occurred of trying to solve the interference problem in the supersonic part of the transonic Mach number range. The first attempts were directed, not without some success (refs. 3 and 4), toward prevention of the bow-wave reflection responsible for the most evident interference effect. Indeed, it was sometimes supposed that a "nonreflecting" wall, or a wall that would not reflect the bow wave, would eliminate the interference. More careful consideration indicated the possibility of other types of interference due not to reflection of disturbances from the model, but to a failure of the bounded wind-tunnel stream to represent the constraints imposed by infinite flow to which the wind-tunnel results must be applied.

Some effects of the boundary layer on the operation of "shock absorbing" walls were very soon apparent (refs. 3, 5, 6, 7, and 8), and the general complexity of the problem had to be faced when an attempt was made to design a practical wind tunnel with minimum interference in the supersonic range (see ref. 5).

The present report is concerned with the general nature of the supersonic interference. These problems are investigated by comparing flow fields about a model enclosed between appropriate walls with the infinitely extended flow about the same model. The calculations were made by means of the characteristics method. (See ref. 9.) This method of investigation is for theoretical purposes preferable to wind-tunnel testing in that it permits more freedom in choice of wall boundary conditions and eliminates the obscuring effect of the boundary layer. A qualitative estimation of the effects of the boundary layer is made by comparing the results of this study with the results of a similar experimental study presented in references 5, 6, and 8.

SYMBOLS

$C_{D,t}$	drag coefficient of model in tunnel
$C_{D,ff}$	drag coefficient of model in free field
C_p	pressure coefficient
D	pipe or hole diameter
p_t	total pressure

k_n	defined in equation (6)
$k_1' = 2K_1/V$	
K_1	porosity factor, $1/k_1$
K_s	porosity factor to remove shock
m	number of tubes per unit wall area
M	Mach number
Q	volume rate of discharge
$q = \frac{1}{2}\rho V^2$	
t	thickness of wall
V	velocity
x,y	coordinate axes
β	ratio of open wall area to total wall area
μ	viscosity of air
θ	flow angle
ρ	density
Subscripts:	
a,b,c	location of points in characteristic system
h	properties of flow through a hole in the wall
l	local
r	reference
s	immediately downstream of the nose shock
x	x component at point (x,y)

[redacted]

0,1,2, . . . n	summation indices
∞	free-stream

THEORY OF WALLS CAPABLE OF ABSORBING BOW SHOCKS

Supersonic Wind-Tunnel Boundaries

The use of the characteristic system to calculate the flow field about a model when the flow field is restrained by a wall requires only that a relation be given between the local velocity V and the flow angle θ at the wall and that the location of the wall be given. From a theoretical viewpoint, both conditions can be quite general and need not represent any practical wall. With this viewpoint in mind, it is possible to design a wall which will fulfill some particular condition such as the absorption of a shock wave, the nonreflection of all disturbances, the simulation of an idealized porous or perforated wall, or any other property the designer chooses.

The actual mechanics of the computation of a flow field, once the boundary function of V and θ is known, involves the simultaneous solution of the equation locating the characteristic line which intersects the wall with the equation locating the tunnel wall, and a similar simultaneous solution of the function giving V and θ (see ref. 9) along the characteristic line with the wall boundary function of V and θ.

Conditions for Removal of a Nose Shock

In order to reduce to zero the disturbance set up at the intersection of the nose shock and tunnel wall, it is necessary that the velocity and flow directions immediately following the shock be exactly the same as found in the free field, which is defined in this report to be the flow field which exists when the model is immersed in an infinite field. If this condition is not met, then either an expansion wave or a shock will originate at the intersection of the nose shock and tunnel wall. The intensity of this disturbance is determined by the deviation of the actual condition from the free-field condition. Thus, if the wall is to eliminate the reflection of the shock, it is necessary that the $F(V,\theta)$ which represents the wall be exactly satisfied by the values of V_s and θ_s just downstream of the shock. Such a wall can be said to be nonreflecting in that it does not send a disturbance from the intersection of the nose shock and tunnel wall back to the model.

[redacted]

Nonreflecting Walls

A nonreflecting wall is sometimes loosely defined as a wall that will not show any disturbance in the field arising from the disturbances due to the model. This definition does not yield a unique mathematical relation which can be used in conjunction with the characteristic equations to calculate flow fields.

A definition of a "nonreflecting" wall can be ascertained from examination of the obvious two-dimensional nonreflecting field in which no disturbances are returned to the flow field from the wall. (See fig. 1.) The effects of this wall (or of any other wall) on the flow field can be simulated by replacing the wall with an exterior hypothetical flow field. In the two-dimensional case previously mentioned, the effect of the nonreflecting wall is represented by a hypothetical exterior flow field behind a planar shock. The planar shock must be an extension of the bow shock beyond the wall and must have properties identical to those of the bow shock at the wall. An example of a reflecting wall is the closed-tunnel case, which may be simulated by restraining the interior flow field with a field of infinite velocity and zero flow angle.

Both these examples show several interesting features of nonreflecting walls. It is observed that for the nonreflecting case the disturbances from the model are lost to infinity along the extended lower characteristic lines and hence are not returned to the model (fig. 1), and that no discontinuity in V or in θ appears at the wall location. On the other hand, in the reflecting case, the disturbances are returned to the stream and discontinuities in V and θ exist across the wall. Thus, it appears reasonable to assume that a wall is nonreflecting if no discontinuities in either V or θ occur along the lower family of characteristics in the hypothetical flow field at the position of the wall.

This definition does not result in a single unique expression for a nonreflecting wall because the condition of continuity of V and θ at the wall does not determine the derivatives of V and θ at the wall. Thus the flow field outside the hypothetical wall is not unique, and as a result many nonreflecting walls exist mathematically. The existence of many nonreflecting walls indicates a strong possibility that some of these walls can create severe disturbances, and so the conclusion must be drawn that nonreflecting walls are not necessarily noninterfering walls.

The three-dimensional nonreflecting wall, like the two-dimensional one, may be simulated by an infinite number of hypothetical exterior fields. In order to study and compare the magnitudes of the interference

effects of various nonreflecting walls, three nonreflecting three-dimensional walls were set up for calculation. In the first case a conical-shock flow field was used to simulate the wall, just as the planar shock was used in the two-dimensional example. The second case, called a constant V,θ field, was based on the assumption that the velocity and flow angles were held constant along each characteristic line to the first point of the computed network outside the tunnel. Continuity of V and θ is assured by definition so that this wall is nonreflecting. In the third case V and θ and the first derivatives of V and θ along the characteristic line were assumed to be continuous at the wall. This wall also satisfies the nonreflective condition.

All these walls are mathematical concepts developed to show that a nonreflecting wall is not necessarily a noninterfering wall and that by actual demonstration nonreflecting walls can cause serious interference. Since these walls are mathematical and cannot be experimentally set up without prior knowledge of the free field, it becomes necessary to consider wall boundary conditions which do not generally obey the nonreflective definition but do approximate experimental walls that are capable of absorbing the initial shock even though they may reflect other disturbances.

Porous and Perforated Walls

The porous wall, for which the flow through the wall is assumed to be proportional to the pressure difference across the wall, is nonreflecting at certain points where the free-stream velocity, flow angle, and porosity obey a specific relationship. An extension of the porous wall which is also nonreflecting at certain points is an idealized perforated wall, for which the mass flow through the wall is assumed to be proportional to the square root of the pressure difference across the wall. In either case, the points of nonreflection may be chosen to eliminate the serious reflections, such as those due to the initial shock.

It might be supposed that by elimination of the reflection of the primary shock, the remaining part of the interference could also be reduced to such an extent that the walls would be practically noninterfering. The results of experiments given in references 5 and 6 have shown, however, that shock-absorbing porous walls will reflect disturbances other than the bow shock and will, in general, produce interference. In order to study theoretically the nature of the interference of such walls, it is necessary to express the wall boundary conditions as functions of velocity and flow angle.

The function of V and θ which expresses the influence of the porous wall on the stream is derived in the following manner. First, in order to obtain the ratio between the pressure across the wall and the flow through the wall, it is necessary to know the pressure at the wall in terms of the velocity. If V_x is the x-component of the local velocity at a point in the flow field and V_∞ is the reference, or free-stream, velocity, the linearized pressure coefficient may be expressed by

$$C_p = -\frac{2(V_x - V_\infty)}{V_\infty} \tag{1}$$

If V_l is the total local velocity at the point x, then $V_x = V_l \cos \theta_l$. On the assumption that θ_l is small, $V_x = V_l$ and thus the pressure coefficient at the wall may be approximated with

$$C_p = 2\frac{V_\infty - V_l}{V_\infty} \tag{2}$$

The pressure outside the wall for the porous or perforated case is assumed to be equal to free-stream pressure, and so the difference in pressure coefficient across the wall is equal to the pressure coefficient as given by equation (2). The normal component of the velocity at the wall is $V_l \sin \theta_l$ or, if $\sin \theta_l$ is approximated with θ_l, it becomes $V_l\theta_l$. Thus, the relation between V and θ at the wall becomes, for the porous wall,

$$k_1'V_l\theta_l = \frac{2(V_\infty - V_l)}{V_\infty} \tag{3}$$

where k_1' is a factor that contains the constant of proportionality, the stream dynamic pressure, and the local density. Equation (3) may be rewritten as

$$k_1V_l\theta_l = V_\infty - V_l \tag{4}$$

The perforated wall is obtained from equation (4) by substituting $k_2V_l^2\theta_l^2$ for $k_1V_l\theta_l$, thus making the pressure across the wall proportional to the square of the velocity through the wall and allowing density and other factors to be absorbed in the constant k_2. Then

$$k_2V_l^2\theta_l^2 = (V_\infty - V_l) \tag{5}$$

[redacted]

The addition of equations (4) and (5) results in the relation between V and θ for another theoretically possible wall and suggests that the following power series may be used for the general case in which the pressure difference is a function of the velocity through the wall:

$$V_\infty - V_l = \sum_{n=0}^{\infty} k_n V_l^n \theta_l^n \tag{6}$$

Theoretically, equation (6) and the equation for the velocity along a characteristic line can be solved as simultaneous equations, but obtaining such solutions for values of n larger than 2 is difficult.

Equation (6) presents an interesting possibility in that it does not require that θ_l be zero when the local wall pressure is equal to free-stream pressure, as is the case for equations (4) and (5). A study of the porosity curves of slanted-hole walls presented in reference 8 shows that equation (6) is to be preferred, especially if the constants k_0 and k_1 are used and if the specification is made that the constants k_0 and k_1 be allowed two different values depending on whether the local pressure at the wall is less than or greater than free-stream pressure.

It may be observed that equation (6) contains no requirement that the velocity and flow angle of the hypothetical flow field which would represent the wall be continuous along the characteristic line at the wall location. Thus, porous or other similar partially open walls designed in accordance with equation (6) must to some degree reflect disturbances due to the model with the exception of those at certain design points such as the nose shock or other selected points.

Noninterfering Walls

Since the nonreflecting wall condition was found to be insufficient to insure a noninterfering wall condition, it is apparent that the noninterfering wall must meet more stringent requirements. A tunnel is to be defined as noninterfering if the properties of the flow along the model in the tunnel are identical to those of the flow along the model in the free field. This condition will be satisfied if the flow in the part of the characteristic quadrangle between the wall and the model is the same for the tunnel as for the free-field condition (see uniqueness theorem, ref. 10). A necessary and sufficient condition for the equivalence of the two flows is that the distributions of velocity and flow angles along the wall be identical. This condition is far more stringent

than the nonreflecting condition and for all practical cases requires that a wall be designed with prior knowledge of the free-field flow.

An example of such requirements in wall design may be seen by assuming a variable porosity along the length of a porous wall, so that the parameter k_1 of equation (4) becomes $k_1(\tau)$, where τ is a variable along the wall. Since for the noninterfering condition V and θ are unique along the wall line, $k_1(\tau)$ is also uniquely determined along that line. The porosity distribution is determined by the free field about the model and is different for every different model. Since the porosity distribution is different for each test condition, it would then seem that the problems involved in the design of a generally noninterfering wall would be almost insurmountable.

A corollary to the discussion of the porous-wall example is that the porosity required to absorb a shock is unique for each shock and must be determined from the properties of the particular shock to be absorbed. Thus, it must be possible to vary the porosity of the wall if the effects of a variety of shocks are to be removed.

Approximate Relation Between Porosity Factor k_1 and Percentage of Opening β of a Porous Wall

In order to simplify the relation between k_1 and β, the assumption may be made that the wall consists of a large number of small tubes, that the flow through each tube is uninfluenced by the flow through its neighboring tube, and that the flow through each tube obeys the Hagen-Poiseuille law. This law (ref. 11) states that the volume rate of discharge through a tube is given by

$$Q = \frac{\pi}{\mu t} \Delta p \frac{D^4}{128} \tag{7}$$

where μ is the viscosity, t is the thickness of the wall or length of the tube through the wall, Δp is the pressure across the tube, and D is the diameter of the tube. In order for this law to be valid the Reynolds number of the tube $\rho V_h D/\mu$ must be less than 2,000, ρ being the density of the fluid, and V_h the velocity through the tube.

In applying this equation to a tunnel wall, it is necessary to know the pressure difference Δp across the tunnel wall. The pressure coefficient on the inside of the wall is given by equation (2):

$$C_p = \frac{2(V_\infty - V_l)}{V_\infty}$$

Now assume static or free-stream pressure on the exterior of the tunnel. Then, since C_p is equal to the local pressure less the static pressure, divided by q, Δp is given by

$$\Delta p = \rho_\infty V_\infty (V_\infty - V_l) \tag{8}$$

The substitution of equation (8) into equation (7) gives

$$Q = \frac{\pi \rho_\infty V_\infty (V_\infty - V_l) D^4}{128 \mu t} \tag{9}$$

Now assume that m tubes exist per unit wall area. Since the normal component must flow through the wall the rate of discharge will be $V_l \sin \theta_l$ times the unit area, or with the approximation assumed, the rate of discharge is expressed as $V_l \theta_l$. Then

$$mQ = V_l \theta_l \tag{10}$$

Also, the total tube area in a unit area is equal to $m\pi D^2/4$ or, if the ratio of open to total area is called β, it may be expressed as

$$\beta = \frac{m\pi D^2}{4} \tag{11}$$

The substitution of equation (9) into equation (10) gives

$$V_l \theta_l = \frac{\pi m \rho_\infty V_\infty (V_\infty - V_l) D^4}{128 \mu t} \tag{12}$$

and substitution of equation (11) into equation (12) gives

$$V_l \theta_l = \frac{\beta \rho_\infty V_\infty (V_\infty - V_l) D^2}{32 \mu t} \tag{13}$$

The porosity coefficient k_1 has been defined in equation (4) as

$$k_1 = \frac{V_\infty - V_l}{V_l \theta_l}$$

[redacted]

The use of equation (4) in equation (13) gives the relation between k_1 and β as

$$\beta = \frac{32\mu t}{k_1 \rho_\infty V_\infty D^2} \tag{14}$$

The Reynolds number of the flow through the tube must be less than 2,000, or

$$\frac{\rho_\infty V_h D}{\mu} < 2{,}000 \tag{15}$$

The maximum value for V_h is given in reference 12 as

$$V_{h,max} = \frac{\Delta p D^2}{16\mu t}$$

On substitution of equation (8) for Δp,

$$V_h = \frac{\rho_\infty V_\infty (V_\infty - V_l) D^2}{16\mu t} \tag{16}$$

However, the average value of V_h, equal to $V_{h,max}/2$, is to be used for the Reynolds number calculation. Thus

$$\frac{\rho_\infty{}^2 V_\infty (V_\infty - V_l) D^3}{32\mu^2 t} < 2{,}000 \tag{17}$$

or

$$D^3 < \frac{64{,}000\mu^2 t}{\rho_\infty{}^2 V_\infty (V_\infty - V_l)} \tag{18}$$

This condition must be met if the wall is to be considered as porous. If it is not met, the dynamic effects of the flow entering and leaving the wall will cause the wall to act more like a perforated wall than a porous wall.

A demonstration of the size and number of holes required for a typical tunnel operating condition is given in the following calculations. Assumed values are as follows:

[redacted]

μ, slugs/ft-sec	4×10^{-7}
ρ_∞, slugs/cu ft	0.002
V_∞, ft/sec	1,200
V_l, ft/sec	1,100
t, ft	1/48

Substituting these values into expression (18) gives

$$D < 0.000763 \text{ foot}$$

So, assume

$$D = 0.0005 \text{ foot}$$

If k_1 is assumed to be equal to 4.0, equation (14) gives for β the value

$$\beta = 0.1111, \text{ or } 11.1 \text{ percent open} \tag{19}$$

and equation (11) gives for m the value 565,800 holes per square foot, which is equivalent to a spacing of 0.016 inch between centers, with a hole diameter of 0.006 inch.

A study of equation (14) shows that with a fixed wall - that is, with β, t, and D fixed - the possibility exists of varying the porosity factor k_1 by adjusting either the velocity or the density of the free stream. However, not much variation in velocity is possible because for a given free-stream Mach number the velocity varies as the square root of the temperature.

Approximate Relation Between Perforation Factor k_2 and Percentage of Opening β of a Perforated Wall

A perforated wall, for which the pressure across the wall is proportional to the dynamic pressure of the flow through the wall, may also be used to cancel the effects of a shock. In order to calculate the perforation factor k_2 required to cancel the shock, it is necessary to make the simplifying assumptions that the velocity through each hole obeys Bernoulli's law and that each hole acts independently of the other holes. No assumption need be made concerning the size of number of the holes; however, if the flow in the tunnel is to be reasonably smooth, the diameter of the holes should be very small compared with tunnel dimensions.

Upon the assumption that the flow through a perforated wall obeys Bernoulli's equation, the velocity through any hole may be expressed as

$$\frac{\rho_h V_h^2}{2} = \Delta p \tag{20}$$

where Δp is the pressure difference across the wall.

It has been shown that if the pressure outside the wall is free-stream pressure, Δp is given by equation (8):

$$\Delta p = \rho_\infty V_\infty (V_\infty - V_l)$$

Thus, upon substitution of equation (8) into equation (20),

$$\frac{1}{2} \rho_h V_h^2 = \rho_\infty V_\infty (V_\infty - V_l)$$

If the density in the hole is assumed to be equal to free-stream density,

$$V_h = \sqrt{2V_\infty (V_\infty - V_l)} \tag{21}$$

Then, the volume rate of flow through a hole of diameter D is

$$Q = \frac{\pi D^2}{4} \sqrt{2V_\infty (V_\infty - V_l)} \tag{22}$$

and, since the volume rate of flow through m holes per unit area must be equal to $V_l \theta_l$,

$$V_l \theta_l = \frac{m\pi D^2 \sqrt{2V_\infty (V_\infty - V_l)}}{4} \tag{23}$$

Now $\beta = \frac{m\pi D^2}{4}$, and k_2 is defined for a perforated wall as

$$k_2 = \frac{V_\infty - V_l}{V_l^2 \theta_l^2} \tag{24}$$

[redacted]

The use of equation (24) in equation (23) results in

$$\beta^2 = \frac{1}{2V_\infty k_2} \tag{25}$$

Consider, instead of k_2, a new nondimensional constant

$$K_2 = \frac{V_l^2 \theta_l^2}{V_\infty (V_\infty - V_l)} \tag{26}$$

Use of this constant in equation (23) gives

$$\beta^2 = \frac{K_2}{2} \tag{27}$$

Equation (27) shows that the perforation factor K_2 of a perforated tunnel is determined by the ratio of open area to total area and is not dependent on tunnel velocity or density.

Porosity Conditions Required for Removing Shocks

It has already been noted that the reflection of a nose shock can be prevented if the wall condition satisfies exactly the interference-free flow-field condition immediately behind the shock. This condition can be calculated for either a porous wall (eq. (4)) or a perforated wall (eq. (24)) by using the values of V_∞, V_l, and θ_l from a set of tables which give the properties of the flow through a shock (see ref. 9). In using the tables of reference 9, it is convenient to convert the Mach number values of the tables into ratios of velocity to limiting velocity and use these ratios in equations (4) and (24).

A set of values of k_1 were thus calculated for the shocks at free-stream Mach numbers of 1.1, 1.2, 1.3, and 1.4. The results of these calculations are shown in figure 2(a), where for convenience in plotting, the reciprocal K_1 of k_1 is plotted against the turning angle downstream of the shock.

In order to obtain a rough approximation of the percentage of opening β required to remove the shock, β was calculated from equation (14) for a transonic tunnel operating with a total pressure of 1 atmosphere and a total temperature of 130° F. The wall was assumed to be 1 inch thick and the tubes through the wall 0.0132 inch in diameter.

The results of these calculations are presented in figure 2(b), in which the values of β that will absorb a shock at a given Mach number are plotted against the turning angle due to the shock. This figure, as well as figure 2(a), shows primarily that a variation of 2:1 is required in porosity ratio K_1 or percentage of tunnel opening β to remove weak shocks at a given free-stream Mach number. The figure also shows that normal or near normal shocks require almost a closed tunnel for absorption.

It has already been shown that the wall porosity can vary with tunnel density. It is possible to show the extent of this variation by applying equation (14) to a tunnel with a fixed percentage of opening in the walls and operating at a constant total temperature. The results of such a variation are better seen in equation (14) if it is rewritten by use of K_1, the reciprocal of k_1, for k_1. Thus,

$$K_1 = \frac{\beta \rho_\infty V_\infty D^2}{32 \mu t} \tag{28}$$

It is seen that K_1 varies directly with the density and, therefore, with the pressure. A plot of the total pressure required for shock cancellation in a 25-percent-open tunnel operating at a total temperature of 130° F is presented in figure 2(c). Since the pressure in a pressure tunnel can usually be varied over a range of pressure ratios of 4:1 to 8:1, these results indicate that a possibility of at least partially absorbing the shock exists for a fair range of Mach numbers.

Since a perforated wall can also satisfy the values of V and θ just behind a shock, the values of β required for shock cancellation for a perforated wall were calculated by using equations (26) and (27) and were plotted against the turning angle due to the shock. The plot is presented in figure 3. Analysis of the curves of figures 2 and 3 shows several differences between the values of β that will remove a shock on a porous wall and the values that will remove the same shock on a perforated wall. While the percentage of opening can, with proper selection of tunnel operating conditions, be chosen to have about the same range, the shapes of the curves are much different. The broad maximum shown in the curves of figure 3 indicates that for a fixed Mach number one value of K_2 or β will absorb or nearly absorb a fair range of shocks. As this value is near maximum turning angle, the perforated wall might be preferred in the two-dimensional tunnel where the turning angles may be fairly large.

[redacted]

PROCEDURE

The methods used in presenting the theory of various walls capable of canceling the effects of shock do not result in equations which represent the interference. The interference was therefore determined by calculating the flow field about a number of tunnel model configurations which represent the various walls studied and comparing these flow fields with the corresponding free field. The flow fields were calculated by applying the characteristic-network methods of reference 9 to a two-dimensional, symmetrical, almost parabolic, 10-percent-thick airfoil, with chord equal to 20 inches and the upper surface given by

$$y = 1 - 0.012340172(10 - x)^2 + 0.0000234017 2(10 - x)^4$$

at a Mach number of 1.4, and to a three-dimensional cone-cylinder model having a 17.5° nose cone on a 0.49000-inch-diameter cylinder at a Mach number of 1.194. All the two-dimensional fields were manually calculated. The free field for the three-dimensional axially symmetric cone-cylinder was manually computed for a previous investigation. The restricted cone-cylinder fields were all calculated in the Bell Telephone Laboratories X-66744 relay computer at the Langley Laboratory. The portion of the free field which was to be compared with the restricted fields was recalculated in the Bell computer in order to eliminate any errors that might have occurred in that region of the flow field.

The two-dimensional flow fields that were calculated are: the free field, a porous wall that absorbed the shock, a porous wall with a value of K_1 1.5 times that necessary to absorb the shock, a perforated wall that absorbed the shock, and a nonreflecting field which consisted of a Prandtl-Meyer expansion over the portion of the airfoil affected by the wall. All the walls were located 4.13962 inches from the center line, giving a blockage of 24.16 percent.

The three-dimensional flow fields that were calculated are: the free field, a porous wall that absorbed the shock, a nonreflecting wall with a conical shock extending to infinity from the point of intersection of the shock and wall, a nonreflecting wall with constant V and θ just outside the wall location, a nonreflecting wall with a linear variation of V and θ across the wall location, a porous wall with a porosity 1.5 times that necessary to absorb the shock, and a differential porous wall with a K_1 value of 0.5438 for outflow at the wall and a K_1 value of 0.2000 for inflow at the wall. Two three-dimensional flow fields were calculated that were restricted by walls having porosity curves suggested by the nature of the experimental porosity curves of a wall with 60° slanted holes given in reference 8.

[redacted]

All the three-dimensional wall conditions were calculated for a field consisting of a 0.49-inch-radius model inserted in a tunnel of 3.508-inch radius, to give a blockage of 1.796 percent. Additional fields were included for the shock-removing porous wall, in which the tunnel radius was 4.991 inches and 6.205 inches and gave blockages of 0.88 and 0.57, respectively.

RESULTS AND DISCUSSION

Supersonic-Tunnel Interference Due to Nonreflecting Walls

Two-dimensional nonreflecting walls.- The two-dimensional flow field about the parabolic airfoil restricted by the nonreflecting wall, discussed in the section entitled "Nonreflecting Walls," may be easily calculated if it is remembered that no disturbance due to the planar shock can occur on the model. The flow is therefore a Prandtl-Meyer expansion downstream of the first point on the model influenced by the wall.

The pressure-coefficient distribution due to this expansion, as well as the free-field pressure distribution, is presented in figure 4. The difference between the model pressure-coefficient distribution restricted by the planar shock wall and the free-field pressure coefficient is so small that the differences cannot be detected in the curves of figure 4. These differences are of the order of 0.3 percent of the free-field velocity and are indicative of the degree of disturbance that is due to the curvature of the shock in a two-dimensional flow field containing a thin sharp-nosed model.

Free-field characteristic network.- The characteristic network of the free field for the cone-cylinder model is given in figure 5 to show the nature of the three-dimensional field being studied. It may be observed that an expansion fan comes off the corner and that the resultant overexpansion must be compressed back to stream pressure by a shock wave in the field. The shock in this field was not computed. Its existence is evidenced, though, by the crossing over of the characteristic lines. It is believed that this condition will approximate the shock closely enough to allow the resultant interference phenomena to be approximated. This net can also be used to determine the points of origin on the wall of the interferences which occur on the model.

Three-dimensional nonreflecting flow fields.- The pressure distributions on the surface of the cone-cylinder model located in a flow field restricted by the three-dimensional walls previously given as examples of nonreflecting walls are presented in figure 6.

[redacted]

Of the three fields investigated, the flow field restrained by the conical-shock wall shows the least interference. The low interference properties are due to the fact that the conical-shock field sets up exterior disturbances which approximate the free-field disturbances. This flow field corresponds to the two-dimensional flow field with a planar shock and so may be considered the three-dimensional equivalent of a Prandtl-Meyer expansion. A measure of the disturbances due to the curvature of the shock can be seen by comparing the difference between the conical-shock field (in which no disturbances due to shock curvature occur) and the free-stream field with the corresponding difference between the two-dimensional planar-shock field and the two-dimensional free field. This comparison gives an indication of the seriousness of the interference problem caused by the focusing effect of three-dimensional tunnels. The seriousness of this effect is magnified even more when the observation is made that the blockage of the two-dimensional tunnel-model combination was 24 percent whereas the blockage of the three-dimensional combination was 1.96 percent.

The second nonreflecting field, calculated by using the constant V,θ wall, showed pressure distributions (see fig. 6) which were similar to those due to the conical-shock field. The pressures were, however, more negative than those due to the conical-shock wall. This effect is believed to be due to the fact that the velocity is higher outside the wall because of the assumed boundary condition than it is for the conical-shock wall, which requires a negative velocity gradient across the wall in the downstream portion of the tunnel.

The nonreflective characteristic of the constant V,θ wall may be noted by observing the concentration of points near the 7-inch station. These points arise from the continuation of the compression lines that intersect the wall near the 5-inch station (see fig. 5). If a shock were reflected, these points would show a discontinuity in the velocity distribution; also, they would not be located in consecutively increasing order with respect to x on account of the crossing of the characteristic lines. This wall is therefore nonreflecting but, nevertheless, does disturb the free field.

The third nonreflecting wall is the continuous-derivative V,θ wall, for which the derivatives of V and θ are continuous across the wall. Though it is nonreflecting, it shows very severe interference due to the nature of the wall itself. This interference seems to be caused by an accumulation of the extrapolation errors of the linear variation of V and θ across the wall. Since the operation of such a wall is independent of any outside influence of the free-stream flow field, such as might, in the case of a porous wall, be provided by the condition of stream pressure outside the wall, the errors remain unchecked and accumulate downstream.

[redacted]

This wall shows the same nonreflectivity pattern as was observed for the constant V,θ wall, as evidenced by the continuity of the cluster of points near the 7-inch station.

Features of flow fields restrained by nonreflecting walls.- The results of the study of nonreflecting walls indicate several interesting features. The concept of a nonreflecting wall was shown to be expressed by a general theorem which permitted many walls to satisfy the definition of nonreflectivity. It was shown in the results that the degree of interference from such walls was highly variable and that a nonreflecting wall was not necessarily a noninterfering wall. A more stringent definition than nonreflection theory is required of a supersonic-tunnel wall if the wall is to have negligibly low interference properties.

It was also observed that the interference of the wall was dependent on the degree to which the wall or, rather, the exterior field which simulated the wall, approximated free-field conditions. For example, the planar-shock wall or the conical-shock wall, both of which were good approximations to the free-field conditions in that only the effects of shock curvature were deleted, were very good walls with, comparatively speaking, little interference. In contrast to this condition, the continuous-derivative V,θ wall which eliminated all outside disturbances as well as being nonreflecting proved to be so severely interfering that the flow became subsonic downstream. The severe interference was believed to be related to the fact that the wall eliminated all possibility of control from any outside disturbance which approximated the free-field condition. The possibility of causing divergence from free-stream values, such as was shown by the continuous-derivative V,θ wall, led to the conclusion that the definition of a supersonic-tunnel wall should tie the action of the wall preferably to a free-field condition, or at least to a free-stream condition.

The porous wall, although not generally noninterfering, does depend for its action on the pressure outside the wall and this pressure may be controlled and set at free-stream pressure.

Supersonic-Tunnel Interference Due to Porous Walls

Two-dimensional porous walls.- The pressure coefficients on the near-parabolic two-dimensional airfoil in a flow field restricted by various porous walls are presented in figure 4.

Observation of the pressure coefficients due to the porous wall which completely cancels the reflection of the shock shows that this wall is restraining the outflow behind the shock, thereby preventing sufficient expansion for the flow to attain its free-field values. It

is also observed that at the trailing edge the wall is restraining inflow and, hence, causing too much expansion. The indications here are that a porous wall set to remove a shock can cause restraints to the flow which may be serious and certainly cannot be predicted with simple Mach number increment correction.

As is to be expected, the overporous wall allows an expansion wave to follow the shock, and thereby decreases the pressure coefficients. So, also, an underporous wall would cause a shock and, hence, an increase in the pressure coefficients.

It may be observed that the perforated wall has less interference than the porous wall. This may be a fortuitous circumstance. Calculations of additional cases would be required to show whether the perforated wall is generally better than the porous wall. The same phenomena that were observed for the porous wall in connection with too much or too little porosity to remove the shock may also be expected to exist for the perforated wall.

A comparison of the model surface-pressure coefficients in a field restricted by either the porous wall or the perforated wall with the corresponding pressure coefficients in a field restricted by an open tunnel (see fig. 4) gives a concept of the reduction in interference that can be attained in a two-dimensional tunnel by using porous walls. In fact, the interference due to the properly designed porous wall is so small compared with the interference in the open tunnel that it may almost be called negligible. It must be noted, though, that if the porosity is not of the correct value to remove the shock, a serious interference wave can arise from the point of intersection of the shock with the wall. Thus, even though a two-dimensional tunnel can have a relatively small interference pattern, care must be taken to insure that the test conditions are correct or else the interference may become very severe.

Three-dimensional shock-removing porous walls.- The porosity of the shock-removing porous wall for three-dimensional application was determined by substituting the free-field values of V and θ on the downstream side of the shock from the cone-cylinder nose into equation (4). The resultant value was then used as the wall porosity for the entire wall.

A comparison between the pressure distribution over the cone-cylinder model due to this wall and the free-field pressure distribution (see fig. 7(a)) shows that even though the wall removed the shock, it could not absorb the compression wave which immediately follows the shock. The shock-removing porous wall reflects this compression wave as a compression wave. The porous wall also reflects the subsequent expansion wave that arises from the flow around the cone-cylinder as an expansion

wave. The shock which follows the overexpansion due to the corner (see fig. 5) also appears on the model near the 7-inch location and so is not absorbed by the wall (see fig. 7(a)). In this case, as was expected from the theoretical analysis, the constant-porosity wall reflects disturbances from the model and so interference with the flow field.

The reasons why this constant-porosity wall was not noninterfering, and also why constant-porosity walls with constant outside pressure cannot in general be noninterfering, may be seen from examination of figure 8, which presents the porosity as calculated by equation (4) of the various walls studied. The causes of the various reflective interferences and a rough indication of their magnitude can be observed by comparing the porosity of the noninterfering wall, which is a wall with the porosity distribution required for zero interference, with the porosity of the constant-porosity wall. For example, the compression interference observed between the 3.5-inch and 6.25-inch stations (see fig. 7(a)) arises because the constant porosity wall is less porous than the noninterfering wall in the region where θ is positive (see fig. 9(a)) and so a compression wave is reflected. At the point at which the flow direction becomes negative, the porosity of the noninterfering wall changes sign so that the constant-porosity wall becomes too open over a small region. This too-open condition reflects the expansion of the free field as a compression wave. At the end of this region (see fig. 8, the 4.2-inch station) the porosity of the constant-porosity wall becomes less than the porosity of the noninterfering wall and so the expansion wave is reflected as an expansion wave. This wave intersects the model between the 6.25-inch and the 7-inch station. This analysis shows that the various interferences due to the constant-porosity wall can be traced to the differences between the porosity distribution of the constant-porosity wall and the porosity distribution of the noninterfering wall. It seems from the results of this discussion that, in general, walls with a constant-porosity distribution and with constant pressure outside the walls will cause interference with the flow field about the model.

Effects of varying the porosity.- One flow field was calculated with a porosity factor K_1 that was 1.5 times the value necessary to remove the shock or a k_1 factor two-thirds that required to remove the shock. The interference due to this wall may be observed in figure 7(a). The observed strong initial expansion is required to meet the wall boundary condition at the shock-wall intersection point. After this condition is satisfied, the flow shows a compression in the same region in which compression was observed for the shock-removing porous wall. This compression is more severe than for the shock-removing porous wall and the following expansion merely returns the pressure to the free-field level, so that no reflected shock or only a very minor one occurs.

[redacted]

If the wall is not porous enough to absorb the shock, the boundary conditions require that a shock wave be returned into the field. Since a reflected shock greatly complicates the calculation, the field due to a wall with too low a porosity to remove the shock was not calculated.

Interference effects of differential porous walls.- A differential porous wall is defined as a wall that presents different porosities to the flow field, depending upon some given flow characteristic such as the sign of the pressure difference across the wall.

The wall chosen for study was recommended in reference 5 as being superior to the constant-porosity wall because its effective resistance to inflow can be made greater in regions along the wall when the pressure is low. A flow field using such a wall was calculated in order to obtain a comparison of the interference introduced by this wall with that due to the constant-porosity wall. The porosity for outflow was chosen to remove the shock, whereas that for inflow was chosen to be about the average value of the downstream porosity of the noninterfering wall. The results of this calculation are shown in figure 7(a).

It is seen here that the expansion wave which was reflected to the model by the shock-removing porous wall is reflected much more strongly by the differential wall. Also, the far-downstream pressure does not return as rapidly to the free-field pressure. The reason for the excessive expansion wave may be seen by comparing the differential-wall curve of figure 8 with the noninterfering-wall curve. It may be observed that the region in which the differential porous wall reflects the expansion wave as an expansion (that is, the region between the 3.9-inch and 5.7-inch stations where the porosity is less than that of the noninterfering wall) is larger than the corresponding region for the constant-porosity wall. Therefore, it may be expected that a greater reflected expansion wave will occur. The origin of this expansion may be seen by examining figures 9(a) and 10(a) between the 4-inch and 5-inch stations. These figures show that the differential wall seriously restricts the inflow (fig. 9(a)) thereby causing a negative pressure peak (fig. 10(a)) which creates the strong expansion wave that appears on the model.

In view of the fact that, contrary to the results of reference 6, the differential-porous wall resulted in greater interference than the constant-porosity wall, the porosity curves of reference 6 were examined to see whether other phenomena were present which might account for the small interference reported. The plot of pressure across the wall as a function of flow through the wall for the best wall reported in reference 6, the 6-percent-open wall with 60° slanted holes, showed that this wall was capable of sustaining an outflow against a negative pressure gradient. This condition results in a negative porosity value which may also be observed to exist for the noninterfering wall. It was believed

that the simulation of this condition in a theoretical wall might reduce the interference due to the wall.

A reasonable simulation of the slant-hole differential-porous wall of reference 6 can be attained by using equation (6) summed over $n = 0$ and $n = 1$ to represent the wall, provided the values of k_0 and k_1 are allowed to have different values depending upon the sign of the pressure difference across the wall. The wall boundary condition (eq. (6)) thus becomes

$$V_\infty - V_l = k_0 + k_1 V_l \theta_l \tag{29}$$

Two walls meeting the above conditions were set up. One of them theoretically matched the noninterfering wall at three points: (1) the intersection of the shock with the wall, (2) the point on the wall where the pressure gradient is zero, and (3) the point on the wall where the flow angle is zero. The other wall (the experimentally approximated wall) matched the noninterfering wall at only one point, the intersection of the shock with the wall, a necessary distortion of the experimental curve of reference 6 to avoid reflected shock phenomena. Two other points of this wall were chosen to match the experimental values given in figure 6(f) of reference 8. The points chosen were the value of θ where $V_\infty - V_l = 0$, and the value of $V_\infty - V_l$ where $\theta = 0$. The resultant values of k_0 and k_1 for the theoretical matched case were $k_0 = 0.01262$ and $k_1 = 2.69473$ for $V_l < 0.47103$, and $k_0 = 0.00753$ and $k_1 = 1.60779$ for $V_l > 0.47103$. The corresponding values of k_0 and k_1 for the experimentally approximated case were $k_0 = 0.004805$ and $k_1 = 2.16489$ for $V_l < 0.47103$, and $k_0 = 0.009150$ and $k_1 = 4.12265$ for $V_l > 0.47103$. The condition $V_l < 0.47103$ corresponds to a positive pressure difference across the wall and $V_l > 0.47103$ corresponds to a negative pressure difference across the wall.

The cone-cylinder surface pressures, the wall pressures, the wall flow angle, and the porosity function $K_1(x)$ are presented and compared with the corresponding free-field values and corresponding values for a field restrained by a shock-removing wall with constant porosity in figures 7(b), 10(b), 9(b), and 8. It is seen in figure 7(b) that both the differential slant-hole walls reduced the initial compression interference wave but that the same expansion wave appears as was observed with the constant-porosity shock-removing wall. The expansion wave is observed to be of approximately the same strength for the theoretically matched wall as for the constant-porosity wall but is much stronger for the experimentally approximated wall.

[redacted]

These interference waves can be explained from examination of figure 8. The curve for both the theoretically matched wall and the experimentally approximated wall agree rather closely with the curve for the noninterfering wall up to the 3.5-inch station, and therefore it may be expected that the compression observed in the case of the wall with constant porosity will be reduced in magnitude. The large expansion wave observed in the field restrained by the experimentally approximated wall occurs because the porosity of this wall is appreciably less than the porosity of the noninterfering wall between the 3.75-inch and 5.0-inch stations (see fig. 8) and therefore the inflow is restricted and a severe expansion wave is reflected. This wave is more severe than the corresponding wave caused by the theoretically matched wall because the difference between the porosity of the experimentally approximated wall and that of the noninterfering wall is greater than the corresponding difference for the theoretically matched wall.

The experimentally approximated wall does not give the low interference intensities reported in reference 6. A major portion of the difference between the results of reference 6 and those of this paper is believed to be due to alteration of the effective porosity by the boundary layer, especially in regions of inflow through the wall. This subject is discussed in a later section. The interferences of reference 6 are also spread out and not concentrated, because the tests of reference 6 were made in a square tunnel rather than in a circular tunnel. This reduction of intensity of interference due to tunnel shape is further discussed in the following section.

Effects of varying the blockage.- The effects on the interference of varying the blockage (i.e., the ratio of maximum cross-sectional area of the model to cross-sectional area of the tunnel) from 1.796 percent to 0.57 percent are shown in figures 11 and 12. A value of porosity k to absorb the shock was chosen for each case. Model pressures are shown in figure 11, and wall pressures are shown in figure 12.

Analysis of these figures shows that the general nature of the interference effects of the constant-porosity wall was not changed by reducing the blockage. The most prominent effect of reducing the blockage was to shift the location of the interference effects relatively farther downstream on the model. (See fig. 11.) More important, however, is the fact that the intensity of the reflected expansion and compression waves at the position of the model is but little reduced by reducing the blockage. This effect may be expected to be peculiar to a two-dimensional tunnel or to the three-dimensional circular tunnel containing a body of revolution located on the tunnel center line.

The reason for the small reduction in the interference may be seen by examining the flow field about a disturbance located on the tunnel

center line in either a two-dimensional tunnel or a three-dimensional circular tunnel. The effects of this disturbance are transmitted into the field along the characteristic surface originating from the disturbance. These effects are then reflected by the wall into the stream. In both the two-dimensional and the three-dimensional tunnels, the characteristic surfaces of the interference disturbances created at the wall are reconcentrated on the tunnel center line. In the two-dimensional tunnel the disturbances at the wall will be carried to the center with no reduction in intensity, so that changing the tunnel height will cause no change in the intensity of the interference. A three-dimensional tunnel may be expected to act in a similar fashion except that as the tunnel radius becomes larger the disturbance at the wall will become weaker. This effect is compensated by the fact that the wall disturbance is created over an increasing portion of the wall, so that when the entire disturbance is reconcentrated on the center the intensity at the center will remain about constant regardless of the tunnel radius.

This phenomenon of constant intensity of the interference waves regardless of tunnel dimensions cannot be expected to hold for the general three-dimensional tunnel, as the interference characteristic surfaces which originate at the wall will not, in general, be reconcentrated on the center line, but will instead be re-reflected between the various walls and will strike the model many times with weak disturbances. Such disturbances will be spread more and weakened more as the dimensions of the tunnel are increased with respect to the model. This spreading and weakening of the disturbances in a general three-dimensional tunnel helps to account for the fact that the intensities of the disturbances reported in reference 6 are less than those reported herein, as the test results given in that reference involved a cone-cylinder model restrained by a tunnel of square cross section.

Influence of boundary layer on interference of porous walls.- The boundary layer of a tunnel may be considered as a region of reduced velocity enclosing the flow field. Such a region of reduced velocity will contribute a modification to the flow in the direction of an open-tunnel influence. The extent of the modification is dependent on the thickness of the boundary layer, varying from no modification for zero thickness to an open tunnel for infinite thickness.

This analogy shows that the effective porosity of a porous-wall tunnel with a boundary layer present should be greater than the actual porosity of the wall when no boundary layer is present. Since the effective porosity is dependent on the boundary-layer thickness, it may be expected to be appreciably higher in regions where the air flows into the tunnel, because the incoming air greatly thickens the boundary layer. Where the flow through the wall is outward, the boundary layer will be thinner and, as a result, the effective porosity will approach actual porosity.

[redacted]

The changes in interference due to these effects can be fairly large. Reference 5, for example, reports that the inflow through a constant-porosity wall was usually too large and so caused a large downstream compression fan. The theoretical calculations of the present investigation, however, showed that in the absence of a boundary layer the downstream porosity was too small; as a result the inflow was restricted and an expansion wave formed. The indications are, then, that the boundary layer in the experimental tunnel of reference 5 thickened for the inflow and thereby increased the effective porosity to such an extent that a compression wave resulted. This condition was met in reference 5 by using a differential porous wall which restricted inflow more than outflow. The combined effect of both the reduced boundary-layer thickness and the reduced wall porosity resulted in an effective porosity near that required for low-interference properties.

Estimation of interference effects of porous-wall tunnels on drag coefficient and flow angle.- In order to estimate the effect of the interference, the drag of the cone-cylinder model with a flat base was calculated by assuming that the base pressure was equal to the local pressure on the surface of the cylinder as given in figure 7(a). Figure 13 shows the drag-coefficient values obtained by this approximation, and figure 14 shows these values expressed as a percentage error calculated by the following expression:

$$\frac{C_{D,t} - C_{D,ff}}{C_{D,ff}} 100 \qquad (30)$$

where $C_{D,t}$ is the drag coefficient of the model in the tunnel and $C_{D,ff}$ is the drag coefficient of the model in the free field.

Examination of figure 13 shows that the variations in the drag coefficient caused by the various porous walls are appreciable. This point is emphasized in figure 14, which shows the percentage of error introduced into the drag coefficient by the interference of the various walls. Figure 14 shows that the percentage errors for the cases calculated are almost intolerable, varying over a range of -40 percent to 75 percent. Even the best cases, such as the constant-porosity wall set to remove the shock or the theoretically matched wall, produce errors which vary from -20 percent to 25 percent and from 7 percent to 26 percent, respectively. It does not appear to be possible to apply a simple correction for this type of interference.

The fact that the porous walls produce large increments in drag because of their interference effects on the pressure field indicates also that these walls may cause severe interference effects on the flow angle in regions close to the model. The amount of this interference

is shown in figure 15, which presents the increment between the flow angles in the restrained-tunnel fields and in the free field at a radial distance of 1 inch from the model.

The errors observed are appreciable, varying between 1.2° and -1.2° for the worst case calculated and -0.25° to 0.40° for the best case calculated. Errors in the flow angle of the magnitude shown here could cause appreciable changes in such properties as lift and pitching moment of a model if a critical portion of the model, such as a control surface, were located where it would be influenced by the erroneous field. Correction for the effects of this interference seems as complicated as the correction for the drag interference.

SUMMARY OF RESULTS

A theoretical analysis of the supersonic flow about two-dimensional and three-dimensional models restricted by various walls capable of removing the nose shock has shown several interesting features of the interference caused by such walls.

1. A study of nonreflecting walls for both the two-dimensional and three-dimensional cases suggested the possibility that, unless the wall was bound to a free-field property or at least a free-stream property, very severe interference effects could be created by the wall.

2. The noninterfering condition was shown to be far more stringent then the nonreflecting condition. The noninterfering wall was found to require a special distribution of the wall properties which, for most practical cases, are different for every different test condition. The design of the special distribution of wall properties was shown to require a knowledge of the free field.

3. The intensity of interference due to the wall was found to be dependent on the difference between the porosity of the actual wall and the porosity of the noninterfering porous wall. Also, the intensity of interference was found to be sensitive to the tunnel shape, with indication that it would be impractical to make a circular tunnel interference free.

4. The most prominent effect of decreasing the blockage (the ratio of the model cross-sectional area to the tunnel cross-sectional area) was to move the location of the interference waves relatively farther downstream on the model. The intensity of these waves was but little reduced with the reduction in blockage, an effect characteristic of the

three-dimensional circular tunnel. This effect is not expected to hold in noncircular tunnels.

5. The effects of the boundary layer in regions where the flow was inward were found to be so serious that the conclusions indicated by theory concerning the best porous wall conditions for inflow through the wall were rendered wrong. The indications were that the effective porosity over the inflow region of the wall is a combination of the actual porosity of the wall and an effective increase in the porosity due to the thickened boundary layer.

6. Positive or negative interference increments were found to occur for such model properties as drag, lift, pitching moment, and so forth, depending upon the type of wave that would strike critical portions of the model.

7. Supersonic interference effects cannot be expressed as a simple increment such as is used for subsonic blockage correction. The interference is, rather, a complicated function of Mach number, wall porosity, and tunnel and model configurations.

8. No simple solution to the problem of interference at low supersonic speeds appears possible, nor does it appear practical completely to eliminate the interference in any case.

9. In the two-dimensional case, a uniform-porosity wall could be designed for small interference with a particular model and at a particular Mach number, but the interference would become appreciable for off-design conditions.

10. In the three-dimensional axially symmetric case, the porosity distribution required for elimination of the interference is too complicated for practical realization. On the other hand, the required distribution can be roughly approximated by a differential porous wall and the residual interference can be made less evident by use of some test section shape, such as the square, which serves to spread out the disturbances due to the interference.

11. The design of a porous- or perforated-wall tunnel with small interference is complicated by the fact that the porosity distribution required for the elimination of the interference is known only from the free field and by the fact that the effective porosity is largely influenced by the boundary layer, particularly in regions of inflow.

Langley Aeronautical Laboratory,
National Advisory Committee for Aeronautics,
Langley Field, Va., Feb. 12, 1958.

[redacted]

REFERENCES

1. Wright, Ray H., and Ward, Vernon G.: NACA Transonic Wind-Tunnel Test Sections. NACA Rep. 1231, 1955. (Supersedes NACA RM L8J06.)

2. Davis, Don D., Jr., and Moore, Dewey: Analytical Study of Blockage- and Lift-Interference Corrections for Slotted Tunnels Obtained by the Substitution of an Equivalent Homogeneous Boundary for the Discrete Slots. NACA RM L53E07b, 1953.

3. Stokes, George M., Davis, Don D., Jr., and Sellers, Thomas B.: An Experimental Study of Porosity Characteristics of Perforated Materials in Normal and Parallel Flow. NACA TN 3085, 1954. (Supersedes NACA RM L53H07.)

4. Goodman, Theodore R.: The Porous Wall Wind Tunnel. Part III - The Reflection and Absorption of Shock Waves at Supersonic Speeds. Rep. No. AD-706-A-1, Cornell Aero. Lab., Inc., Nov. 1950.

5. Goethert, B. H.: Physical Aspects of Three-Dimensional Wave Reflections in Transonic Wind Tunnels at Mach Number 1.2 (Perforated, Slotted, and Combined Slotted-Perforated Walls). AEDC-TR-55-45 (Contract No. AF 40(600)-620), Arnold Eng. Dev. Center, Mar. 1956.

6. Gray, J. Don, and Gardenier, Hugh E.: Experimental and Theoretical Studies on Three-Dimensional Wave Reflection in Transonic Test Sections. Part I: Wind-Tunnel Tests on Wall Interference of Axisymmetric Bodies at Transonic Mach Numbers. AEDC-TN-55-42 (Contract No. AF 40(600)-620), Arnold Eng. Dev. Center, Mar. 1956.

7. DuBose, H. C.: Experimental and Theoretical Studies on Three-Dimensional Wave Reflection in Transonic Test Sections. Part II: Theoretical Investigation of the Supersonic Flow Field About a Two-Dimensional Body and Several Three-Dimensional Bodies at Zero Angle of Attack. AEDC-TN-55-43 (Contract No. AF 40(600)-620), Arnold Eng. Dev. Center, Mar. 1956.

8. Chew, W. L.: Experimental and Theoretical Studies on Three-Dimensional Wave Reflection in Transonic Test Sections. Part III: Characteristics of Perforated Test-Section Walls With Differential Resistance to Cross-Flow. AEDC-TN-55-44 (Contract No. AF 40(600)-620), Arnold Eng. Dev. Center, Mar. 1956.

9. Ferri, Antonio: Elements of Aerodynamics of Supersonic Flows. The Macmillan Co., 1949, ch. 13.

[redacted]

10. Meyer, R. E.: The Method of Characteristics. Vol. I of Modern Developments in Fluid Dynamics - High Speed Flow, L. Howarth, ed., The Clarendon Press (Oxford), 1953, pp. 77-79.

11. Binder, R. C.: Fluid Mechanics. Prentice-Hall, Inc., 1943, ch. 7.

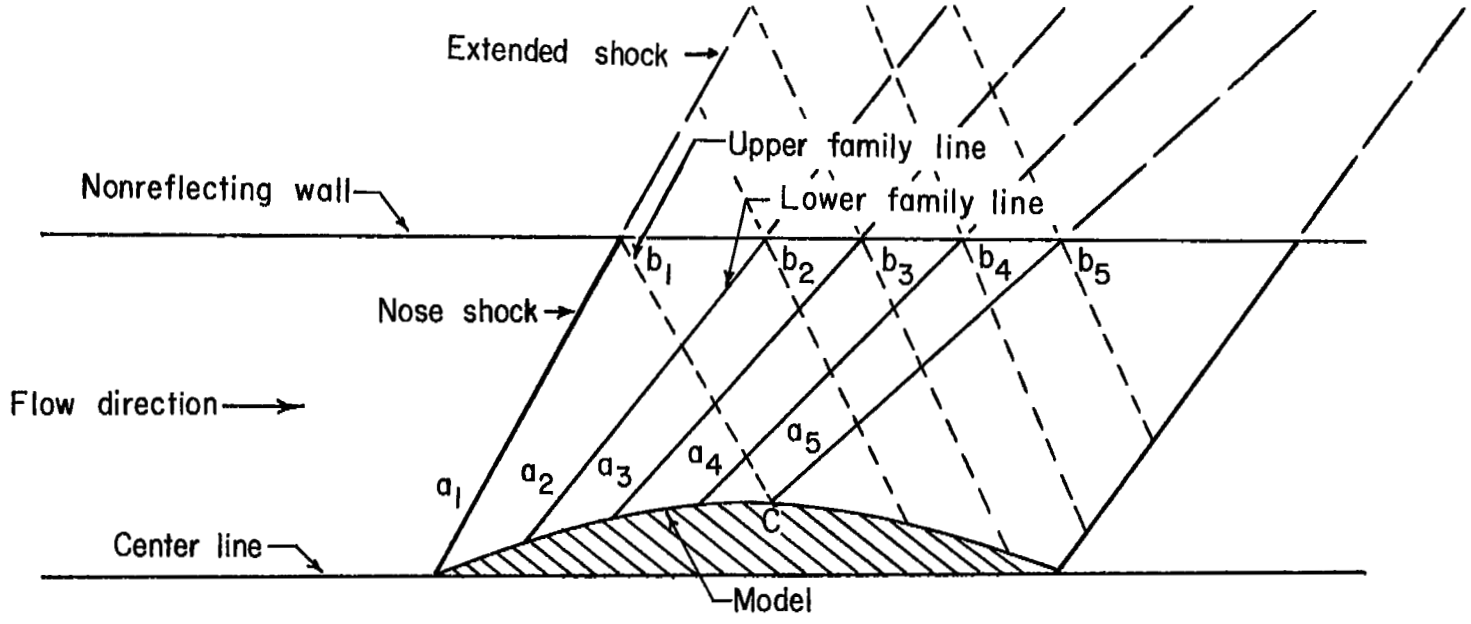

Figure 1.- The supersonic flow field about a two-dimensional model restricted by a nonreflecting wall.

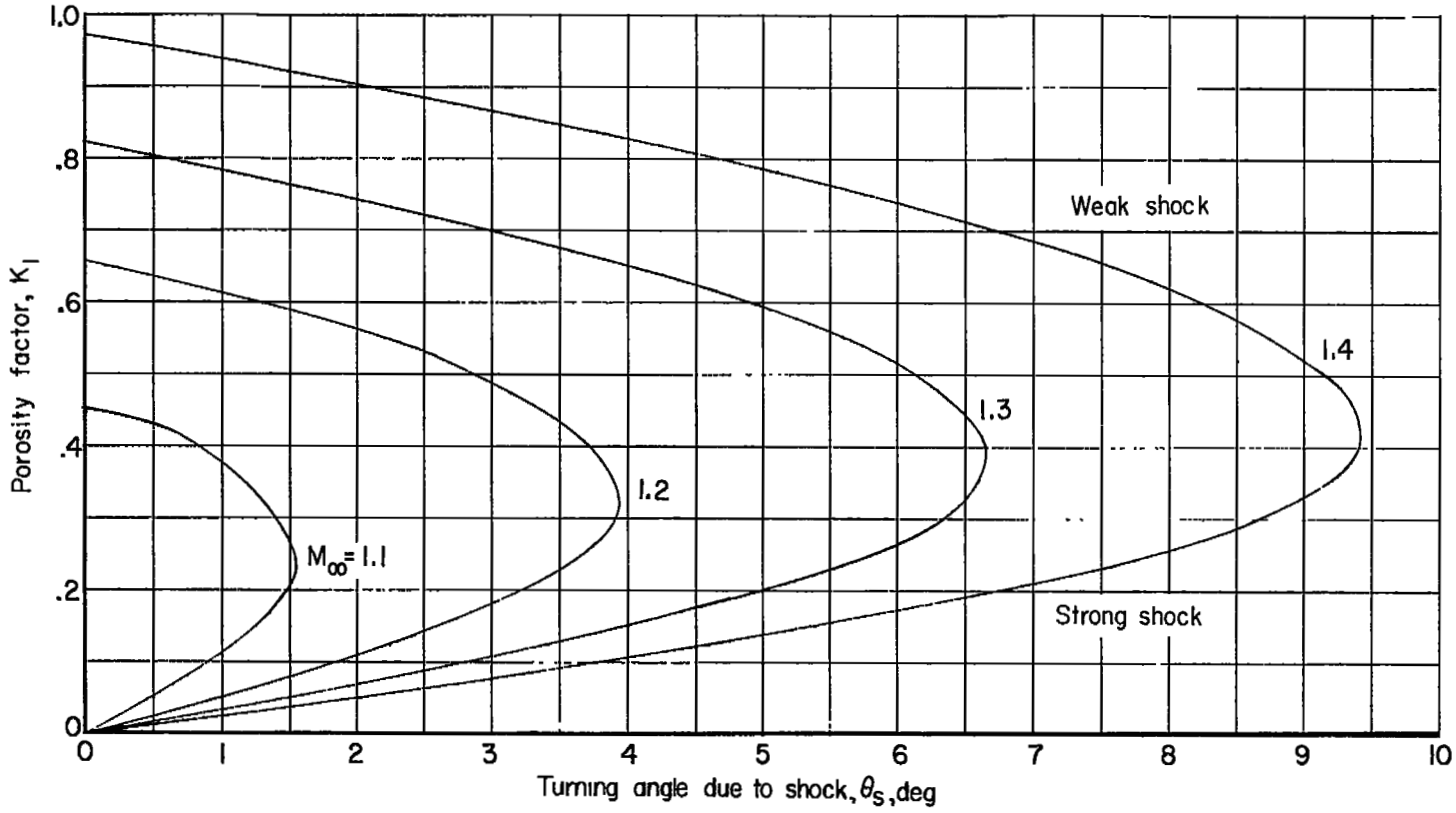

(a) Porosity factor K_1 required to remove various shocks.

Figure 2.- Porous tunnel-wall conditions required to remove various shocks.

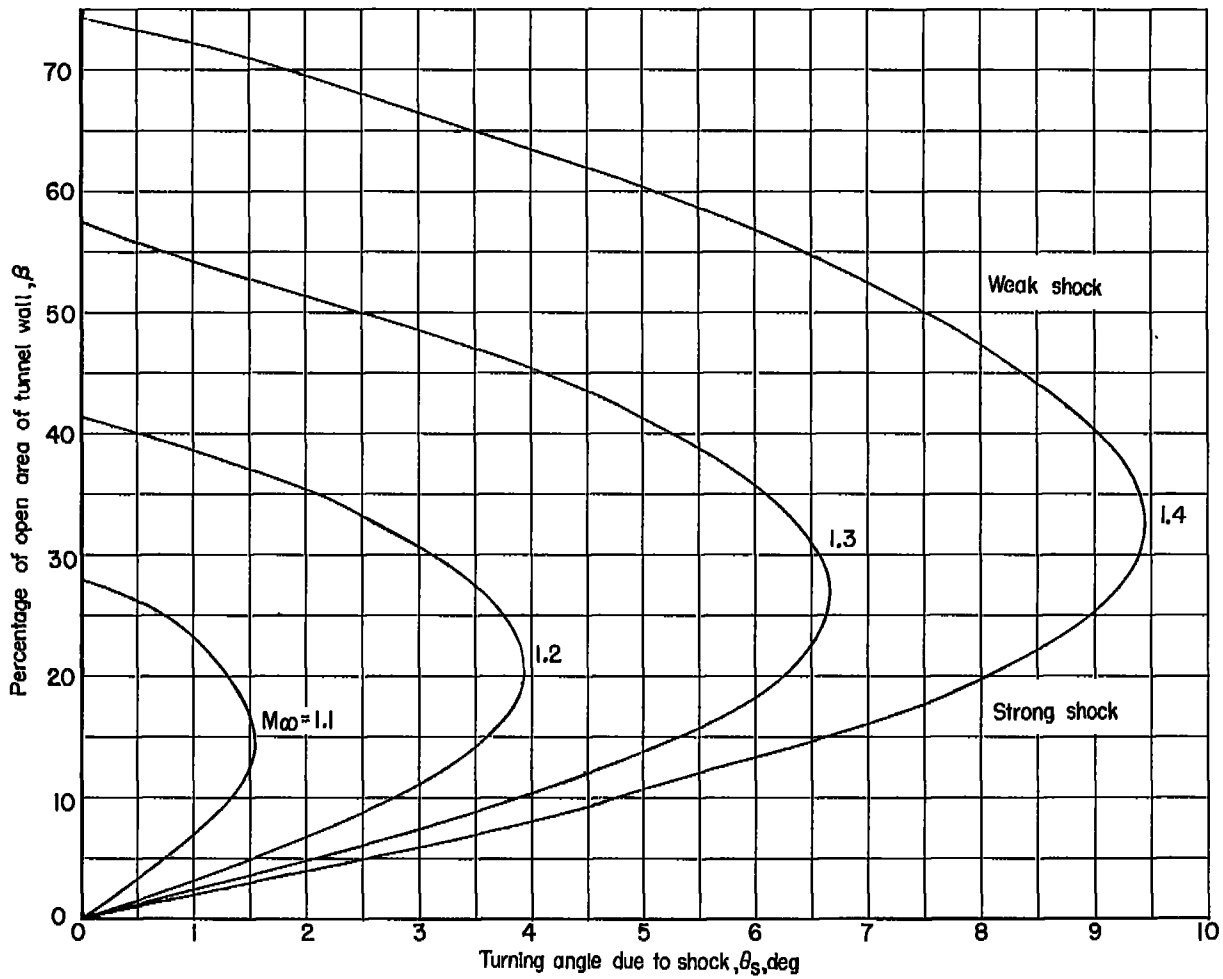

(b) Percentage of open area of tunnel required to remove various shocks. t = 1 inch; D = 0.0132 inch; p_t = 1 atmosphere; total temperature, 130° F.

Figure 2.- Continued.

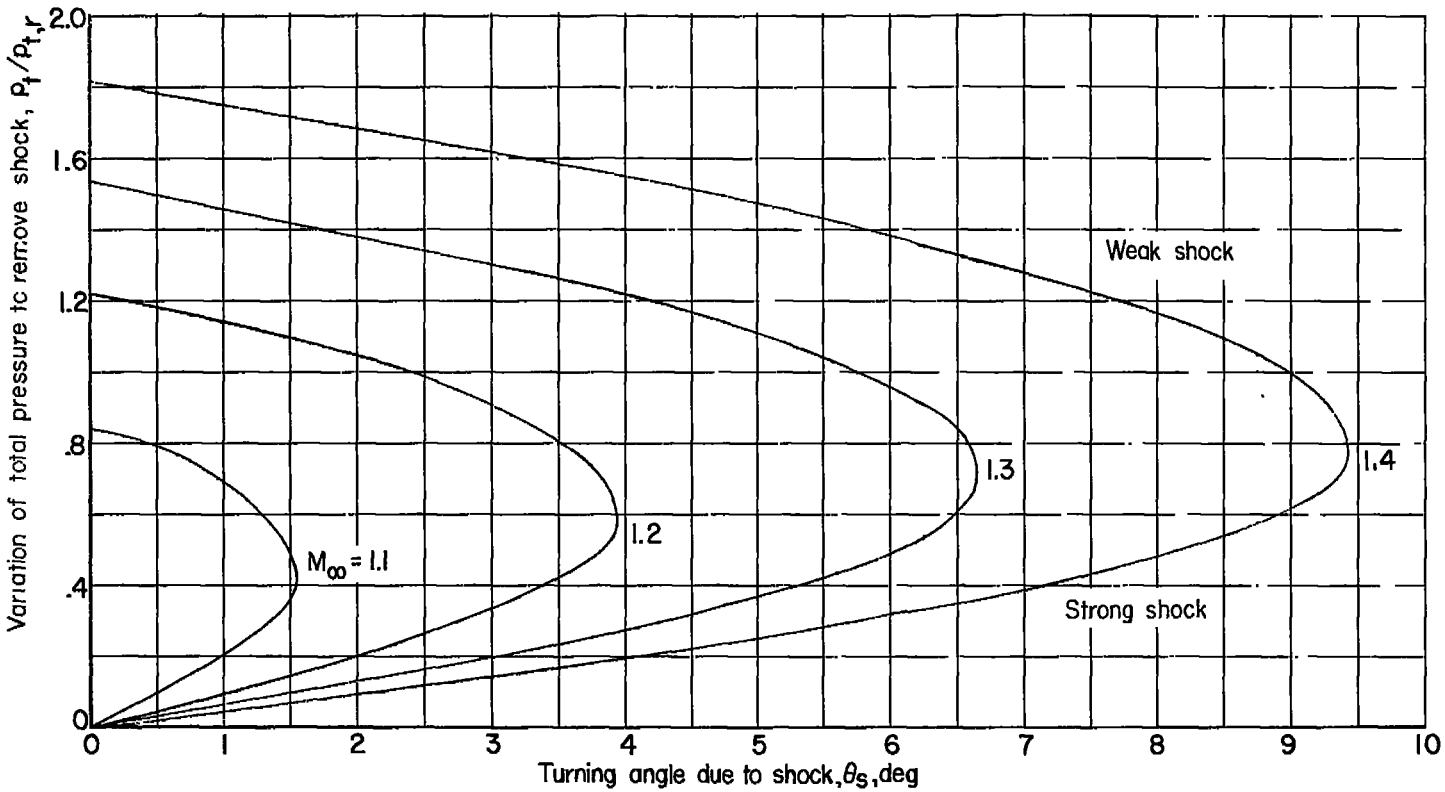

(c) Variation of total pressure required to remove various shocks. β = 25 percent; t = 1 inch; D = 0.0132 inch; $p_{t,r}$ = 1 atmosphere; total temperature, 130° F.

Figure 2.- Concluded.

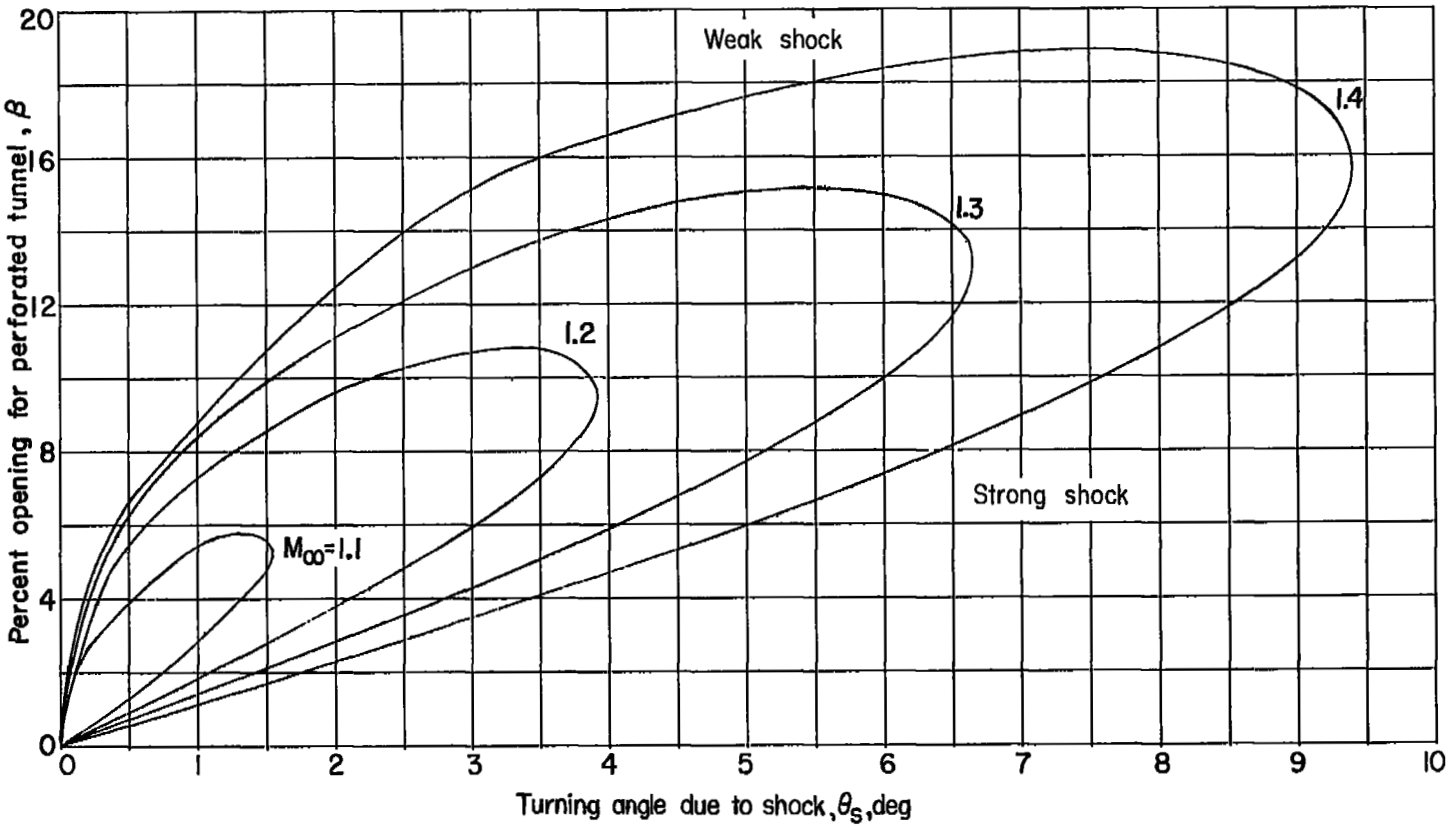

Figure 3.- Percentage of perforation required to remove various shocks.

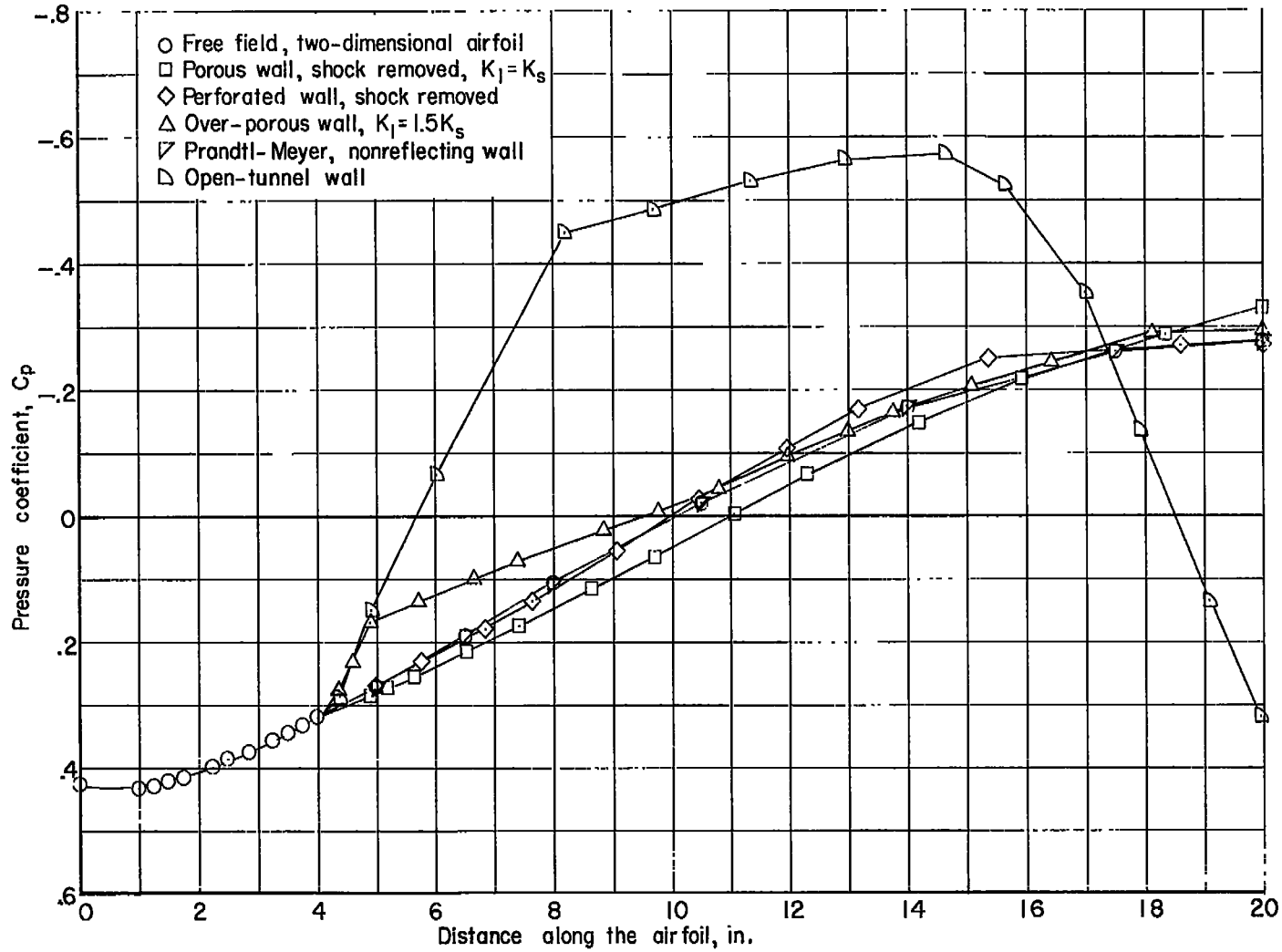

Figure 4.- Pressure coefficients on the surface of a two-dimensional model restricted by various walls. $M_\infty = 1.400$; blockage, 24.16 percent.

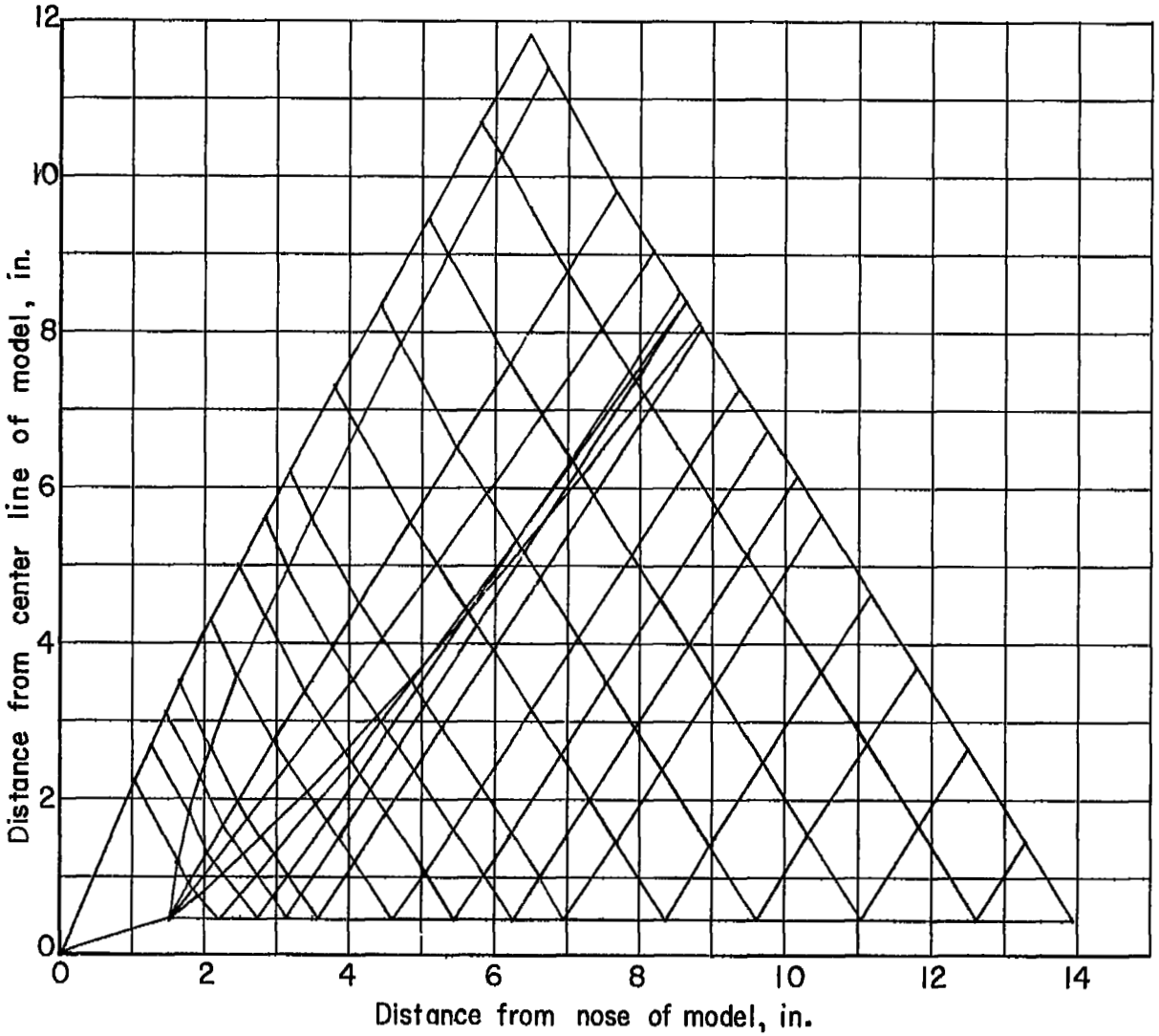

Figure 5.- Characteristic network of the cone-cylinder free field. $M_\infty = 1.194$.

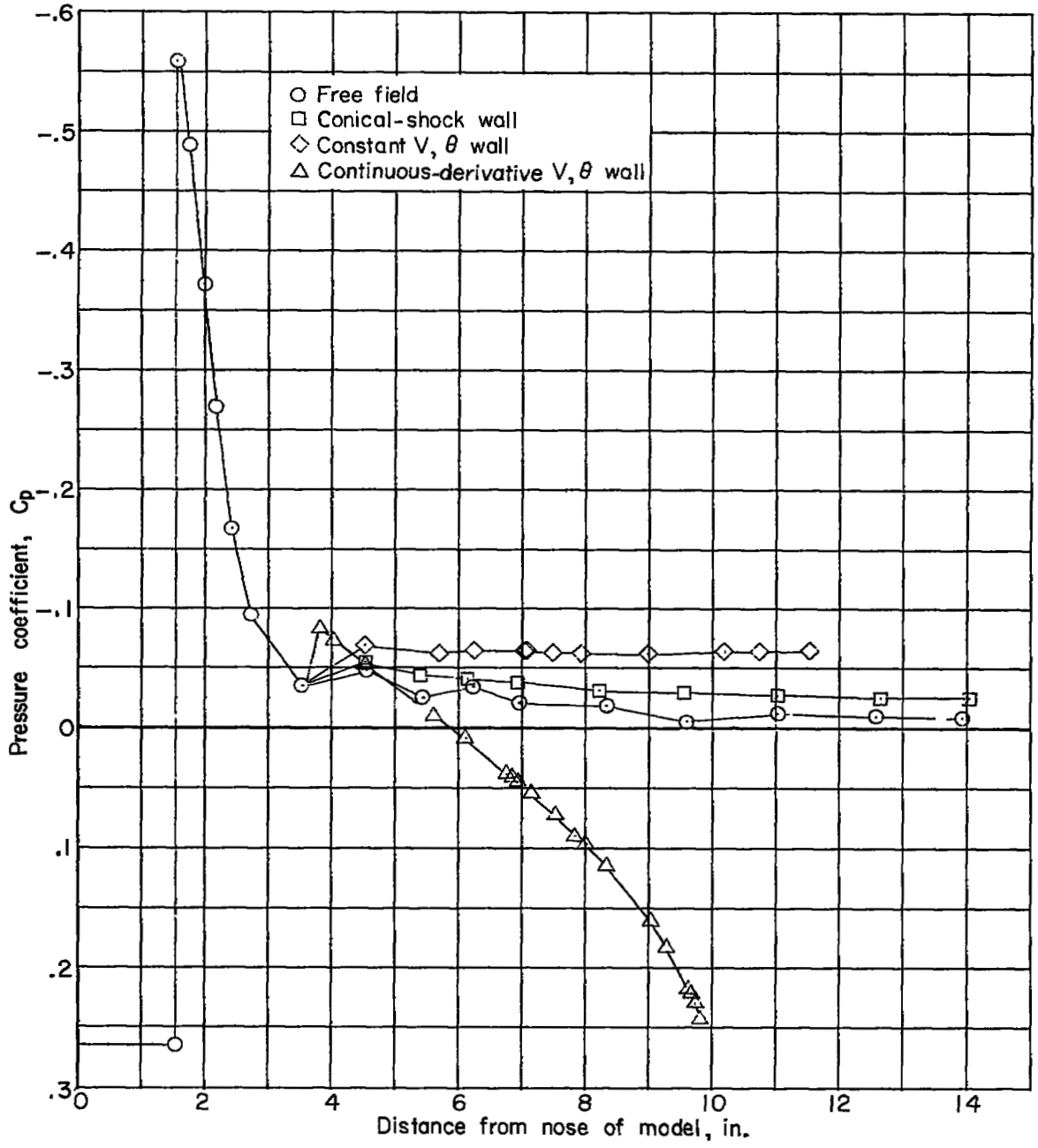

Figure 6.- Pressure coefficients on the surface of the cone-cylinder model due to restraint of the flow by various nonreflecting walls. M_∞ = 1.194; blockage, 1.796 percent.

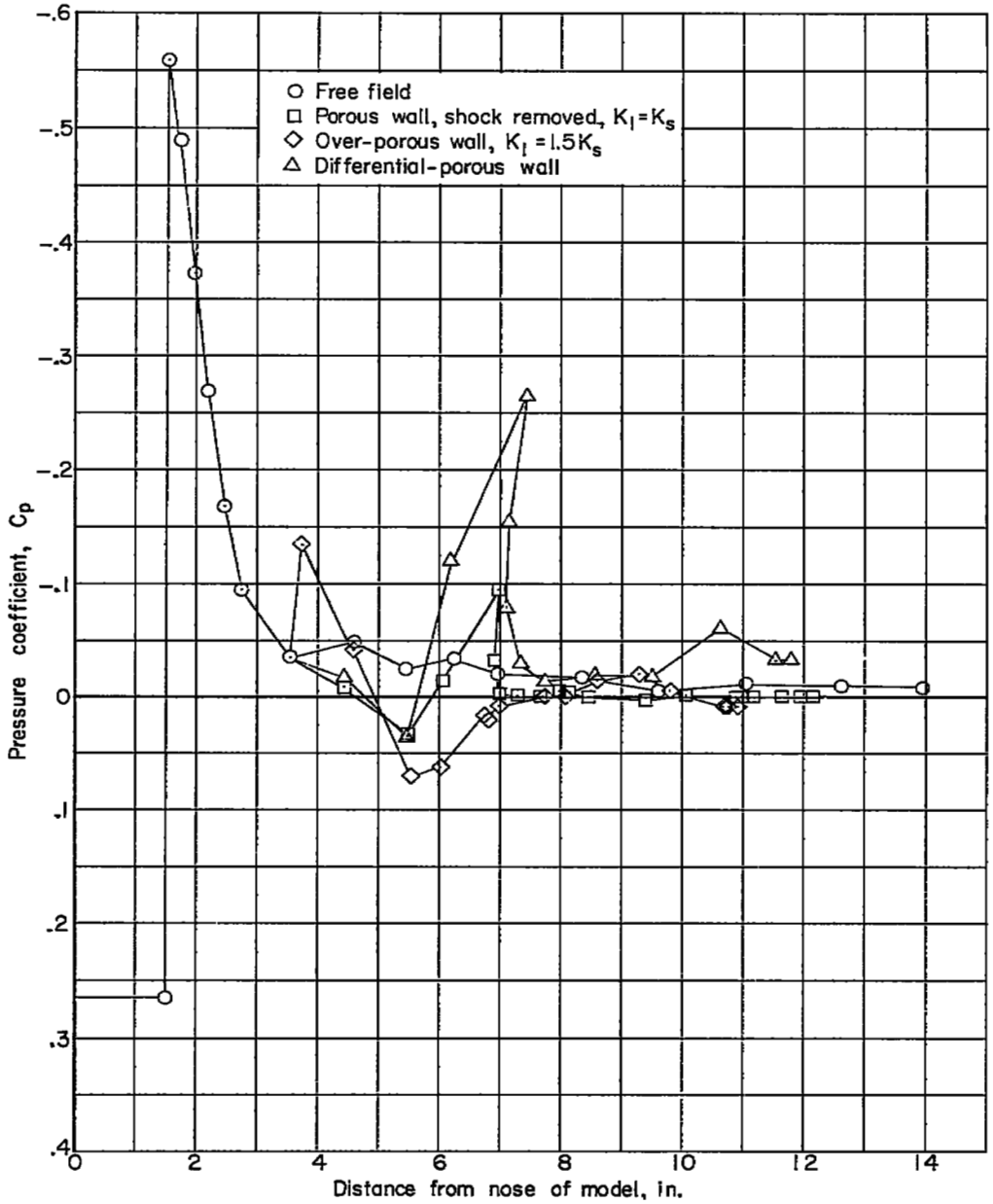

(a) Constant-porosity walls.

Figure 7.- Pressure coefficients on the surface of the cone-cylinder model due to restraint of the flow by various porous walls. $M_\infty = 1.194$; blockage, 1.796 percent.

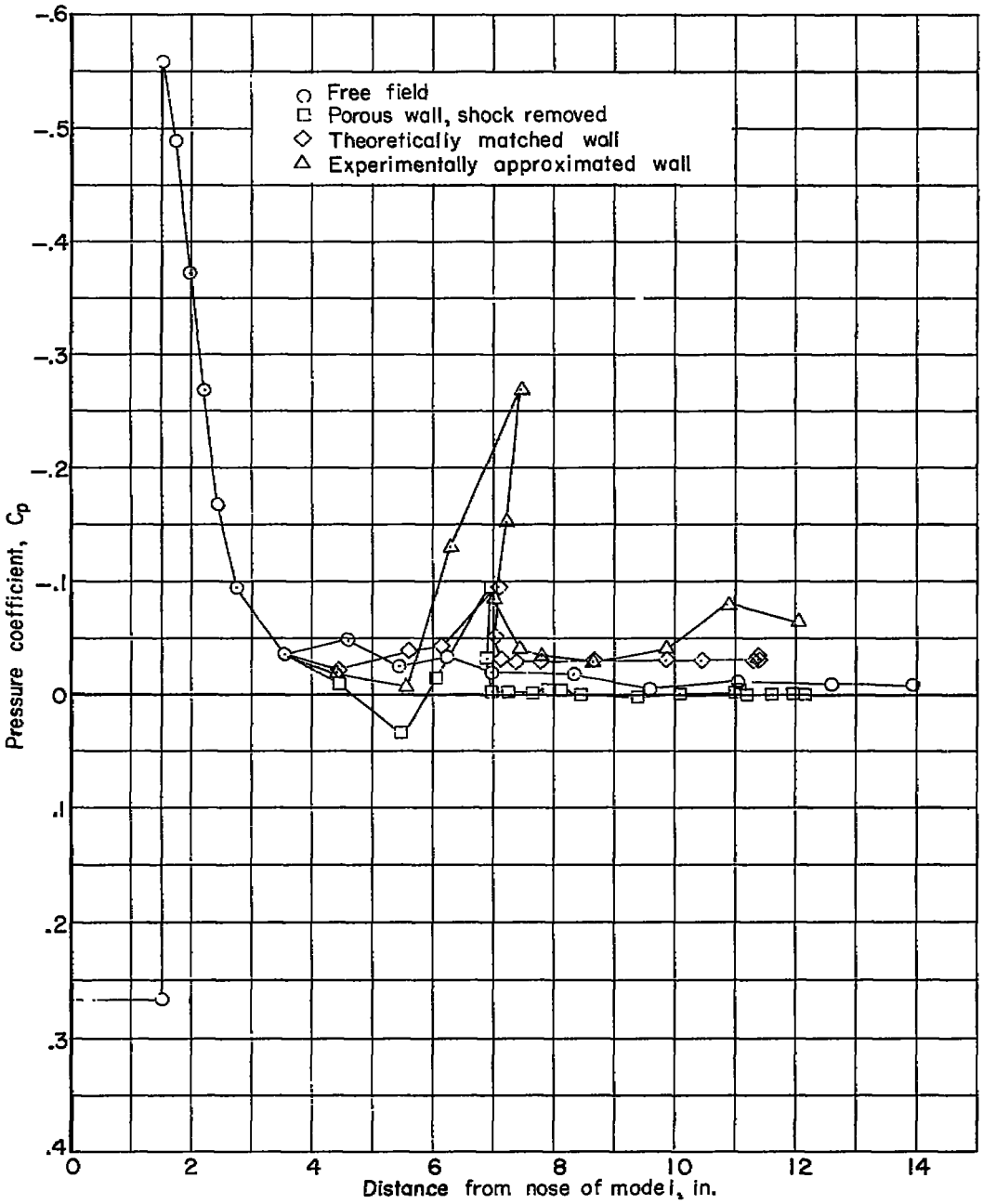

(b) Slant-hole walls.

Figure 7.- Concluded.

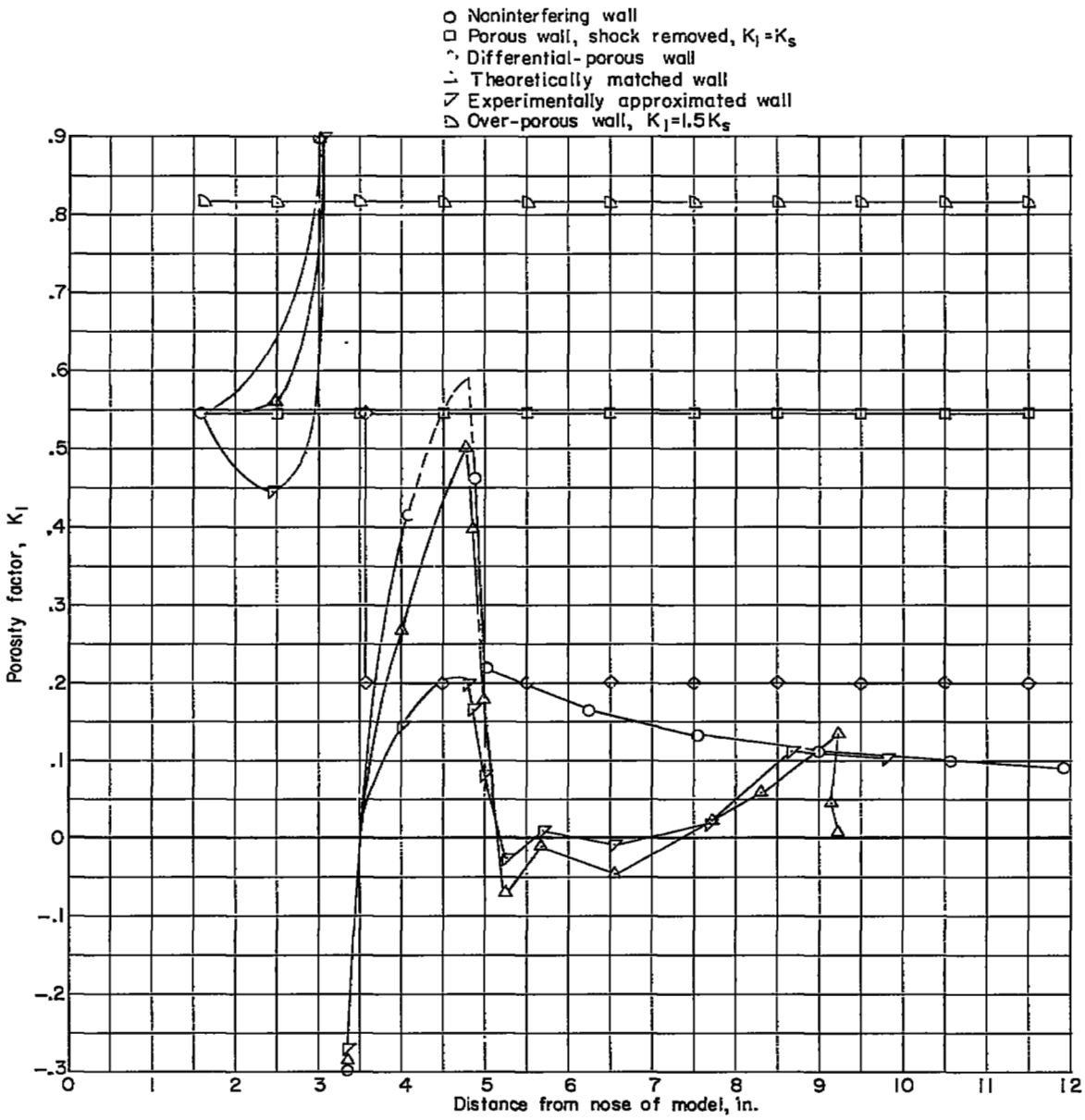

Figure 8.- The porosity factor for various walls.

[redacted]

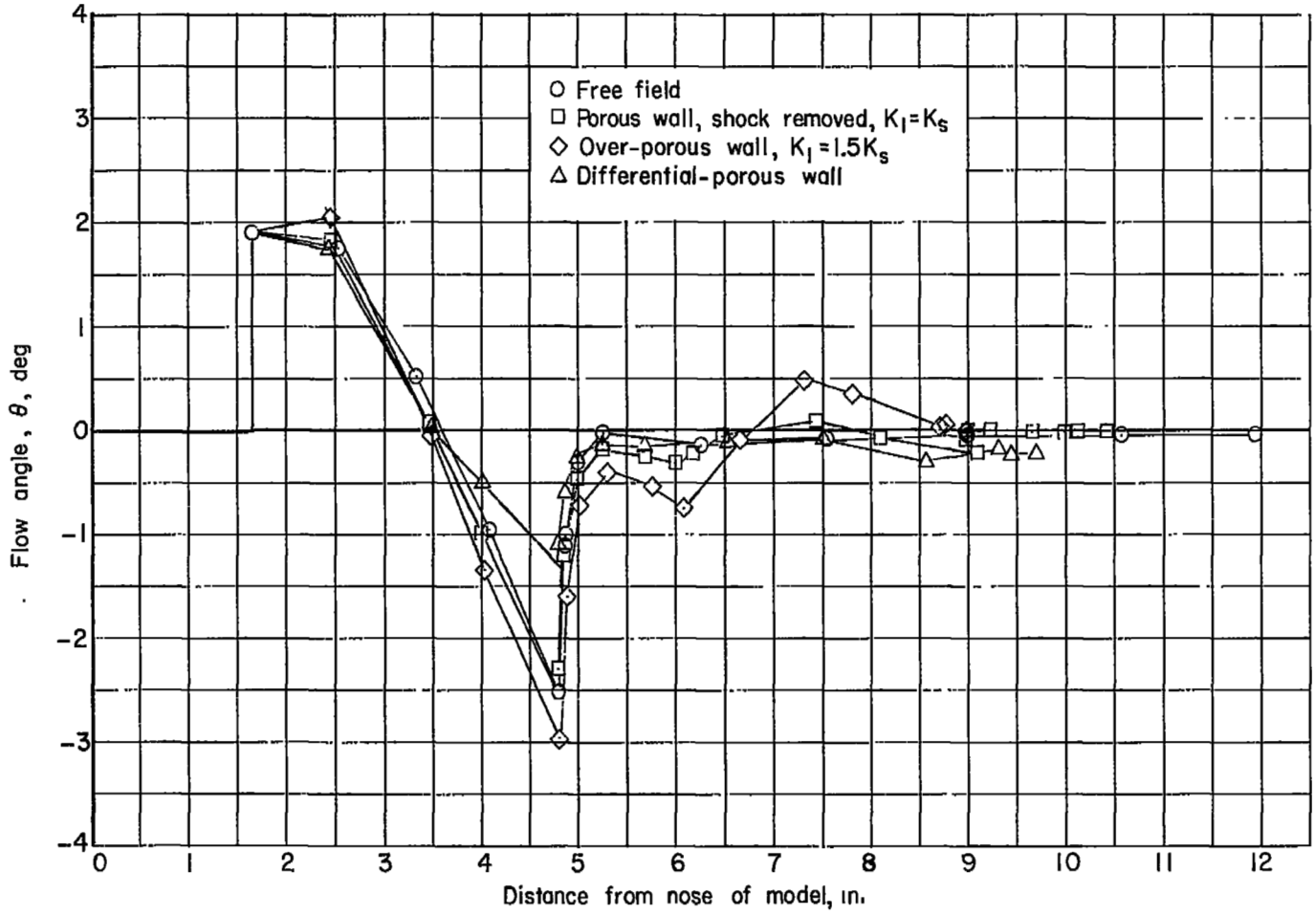

(a) Constant-porosity walls.

Figure 9.- Flow direction at the tunnel wall of the field about a cone-cylinder model restrained by various porous walls. $M_\infty = 1.194$; blockage, 1.796 percent.

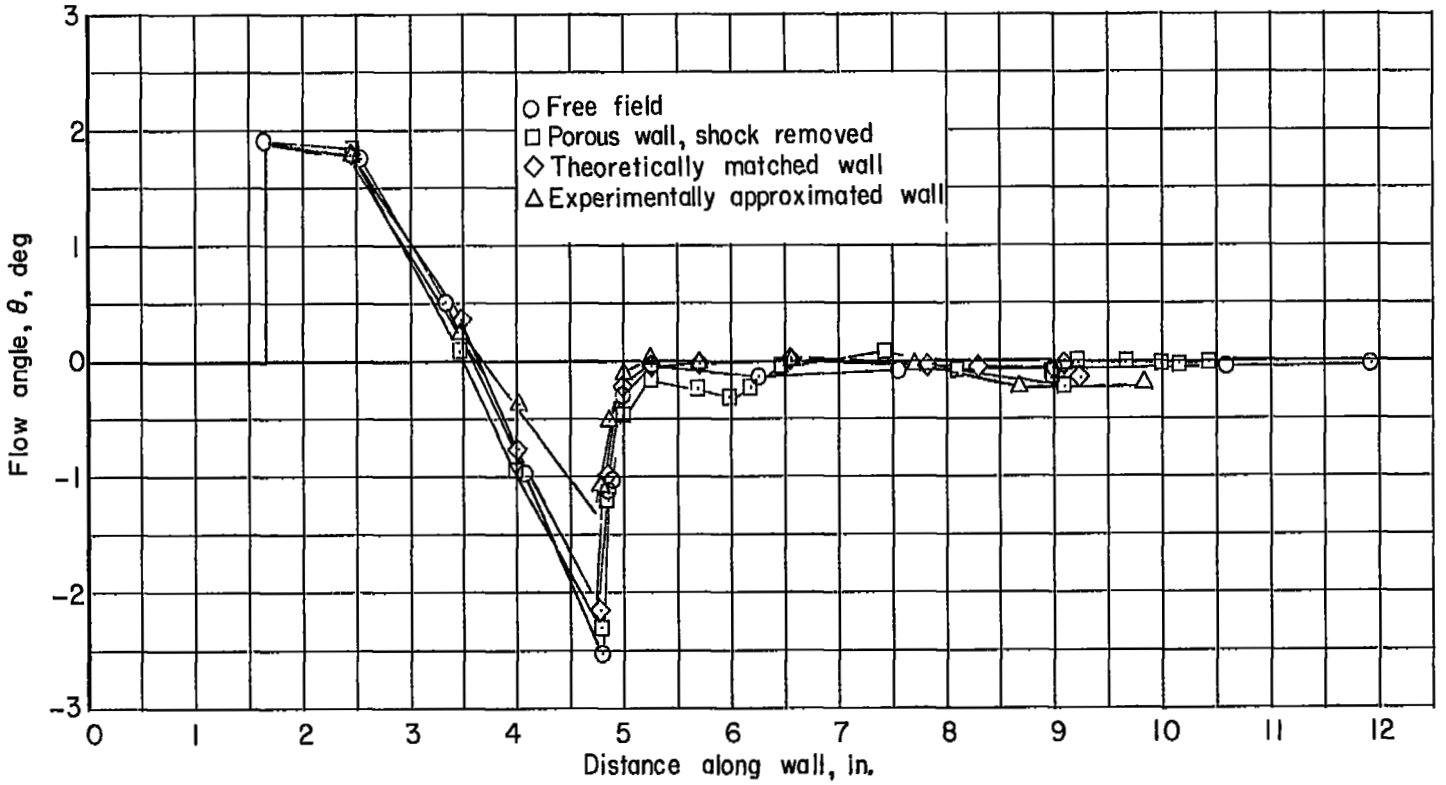

(b) Slant-hole walls.

Figure 9.- Concluded.

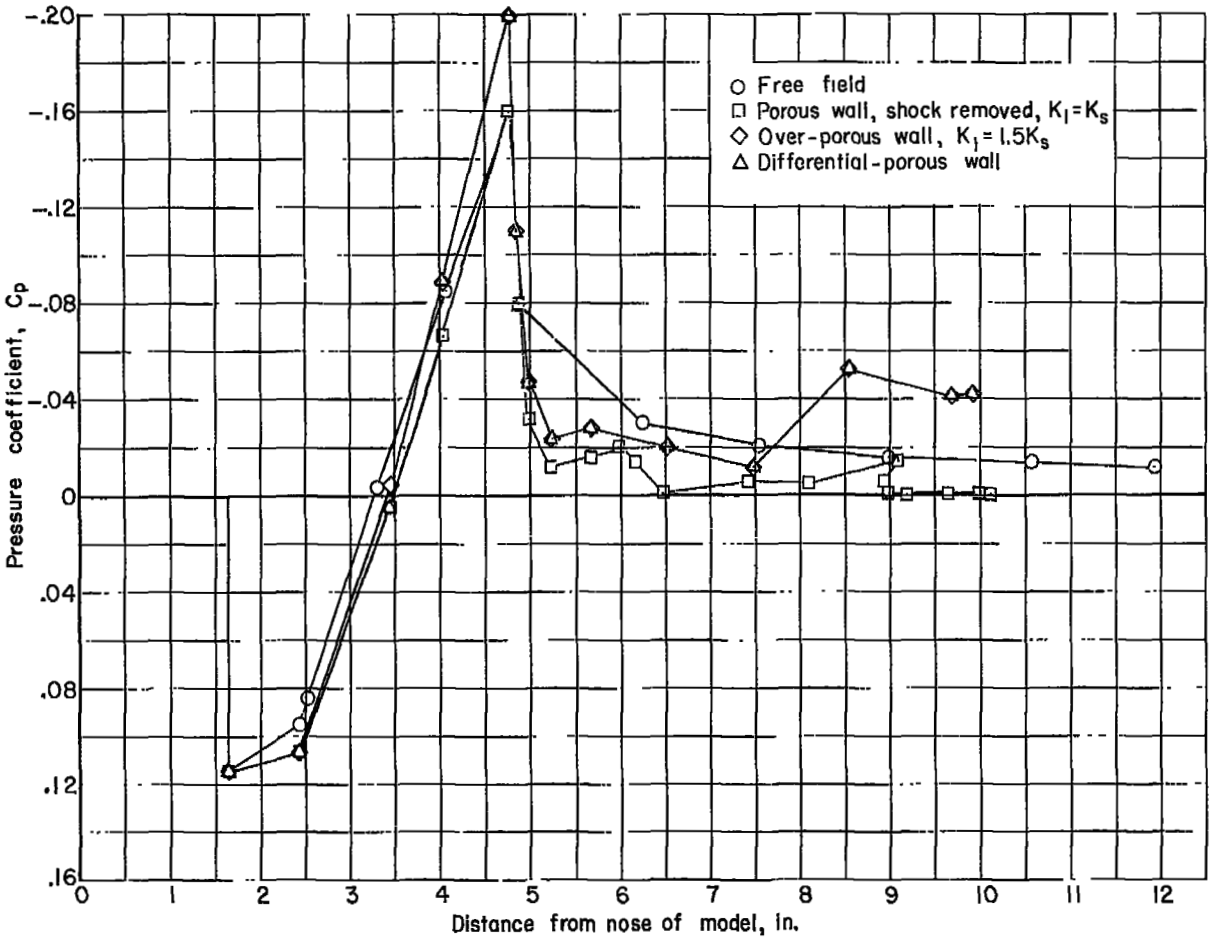

(a) Constant-porosity walls.

Figure 10.- Variation of pressure coefficient at the tunnel boundary for flows about a cone-cylinder model restricted by various porous walls. $M_\infty = 1.194$; blockage, 1.796 percent.

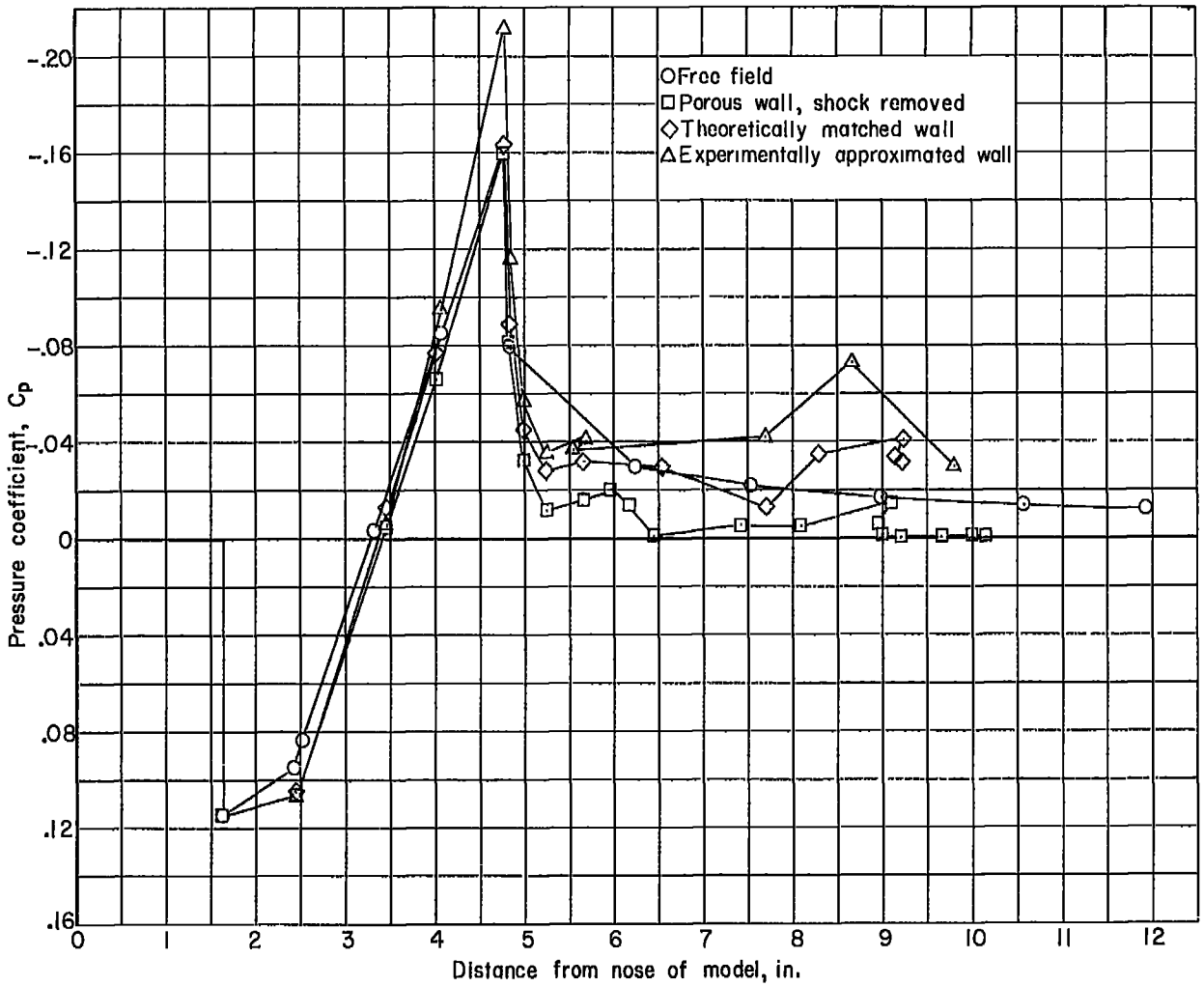

(b) Slant-hole walls.

Figure 10.- Concluded.

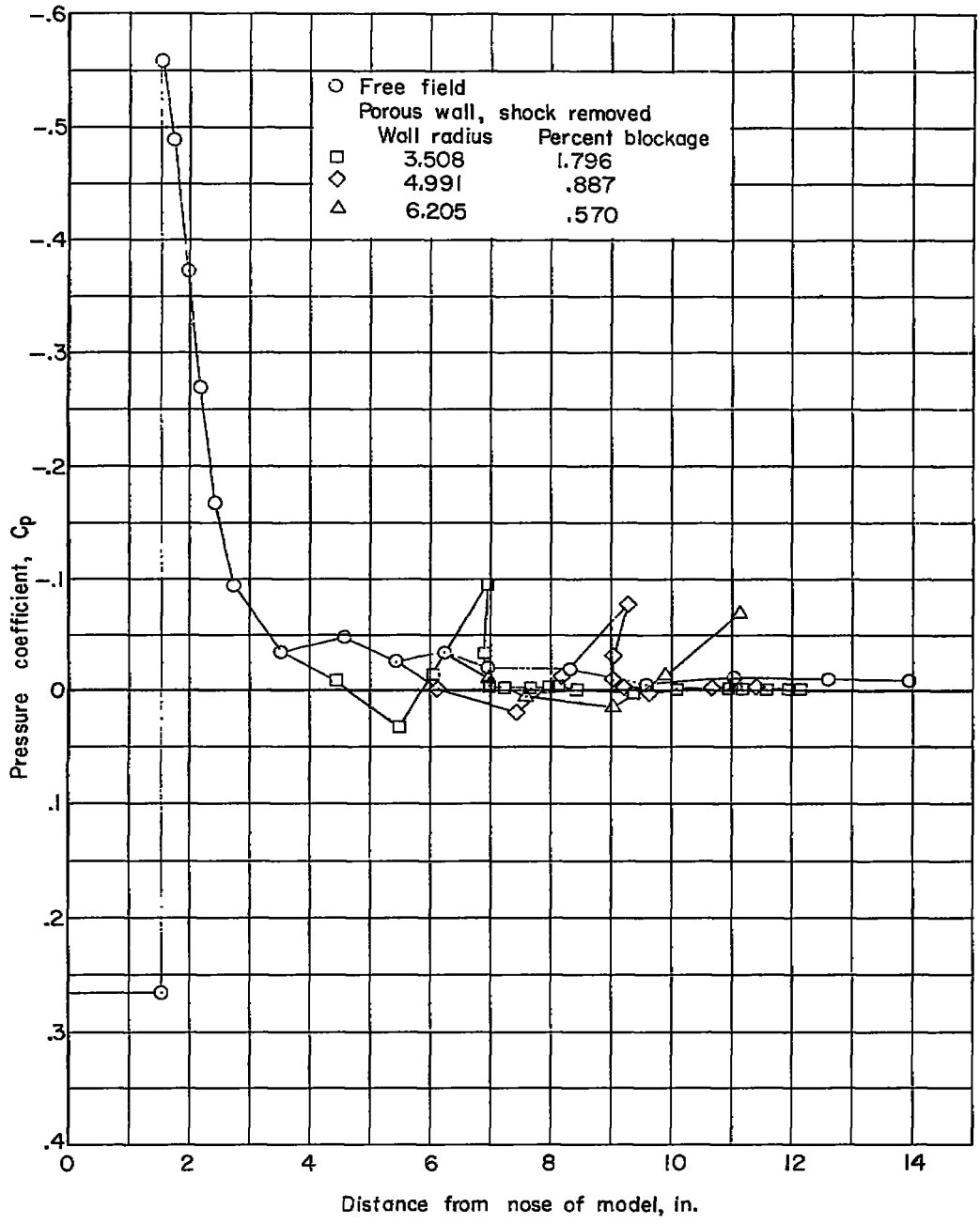

Figure 11.- Variation of the pressure coefficient on the surface of a cone-cylinder model due to changing the blockage of a shock-removing constant-porosity wall.

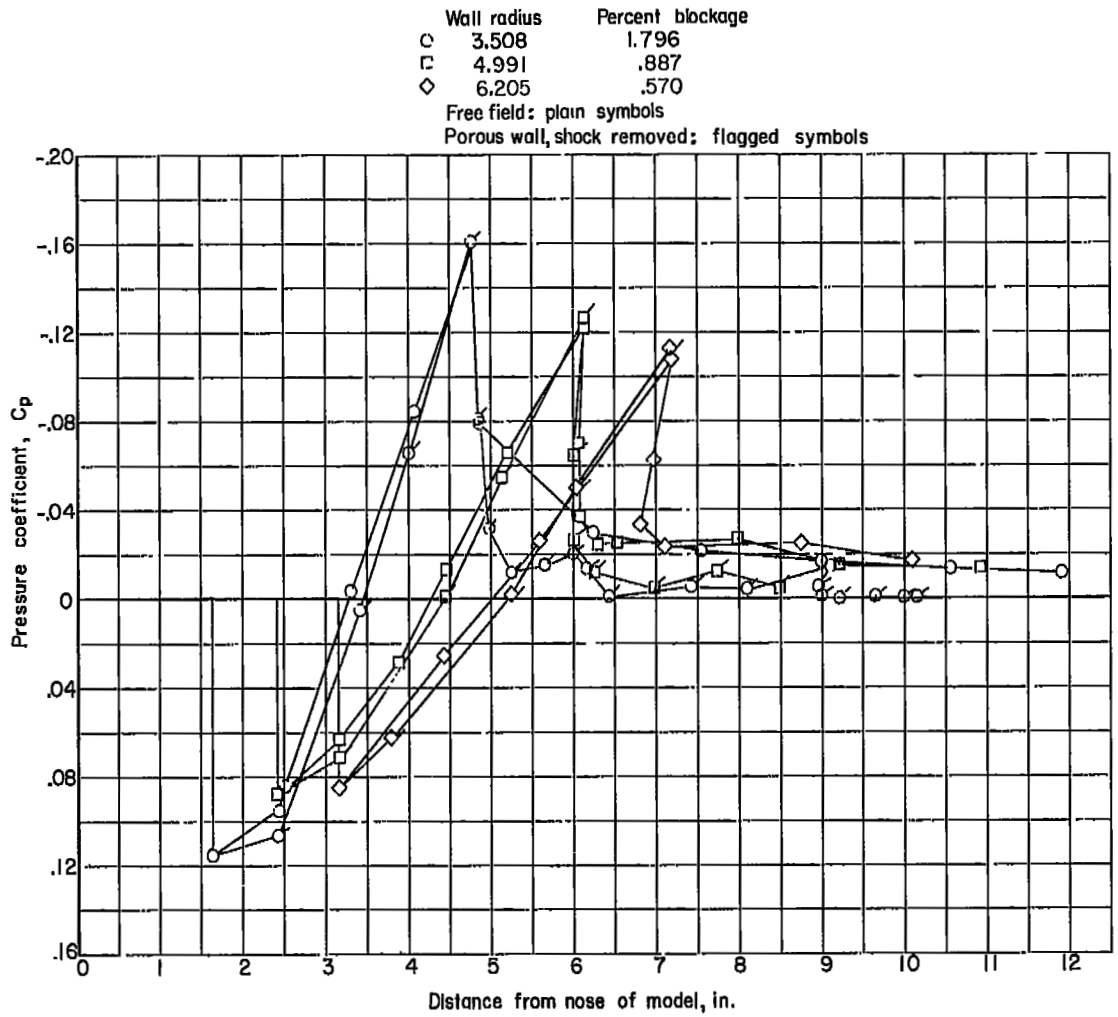

Figure 12.- Effect of percent blockage on variation of pressure coefficient at the tunnel boundary for flow about a cone-cylinder model restricted by shock-removing constant-porosity walls.

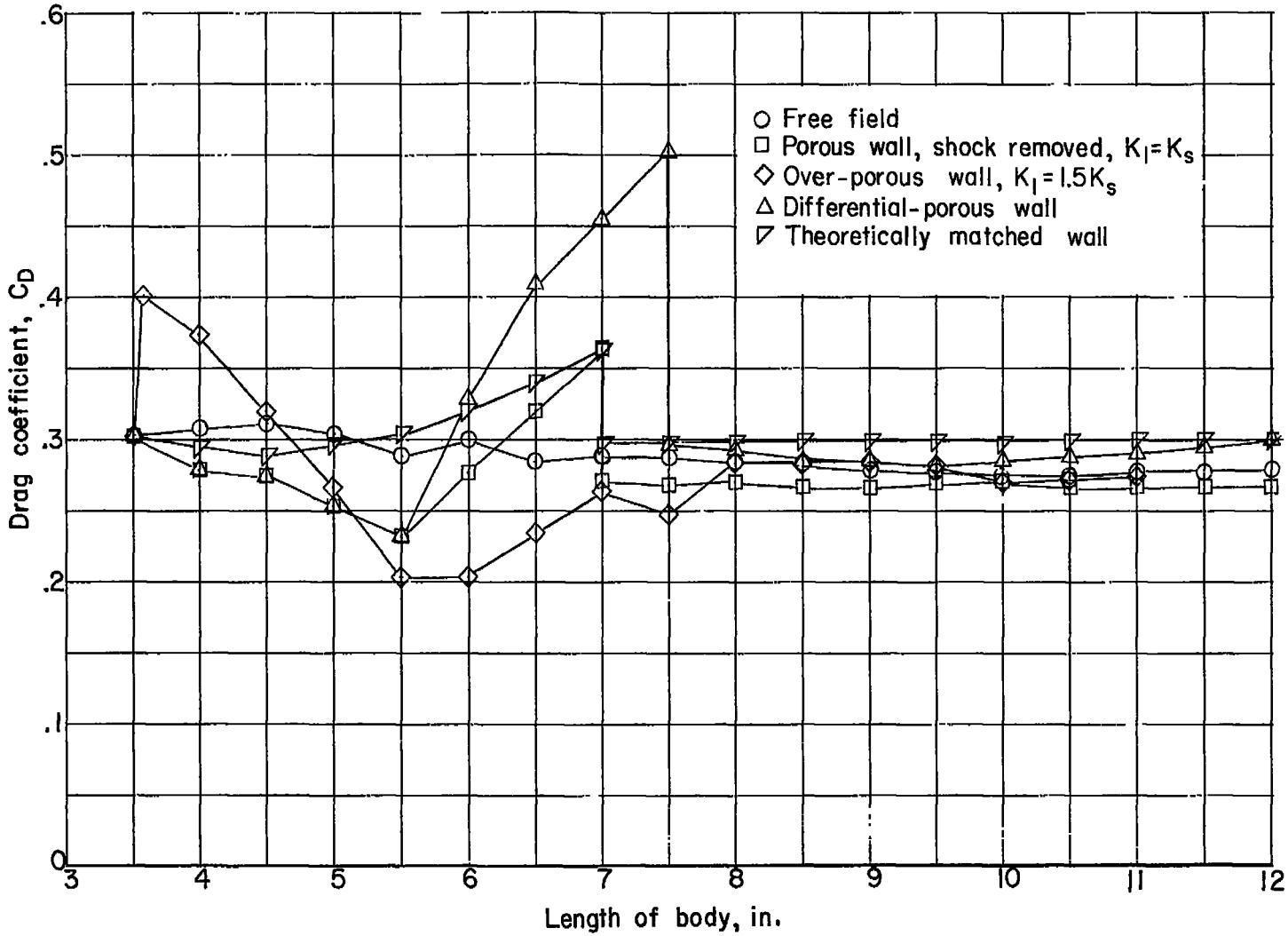

Figure 13.- Drag coefficient of cone-cylinder model with a flat base.

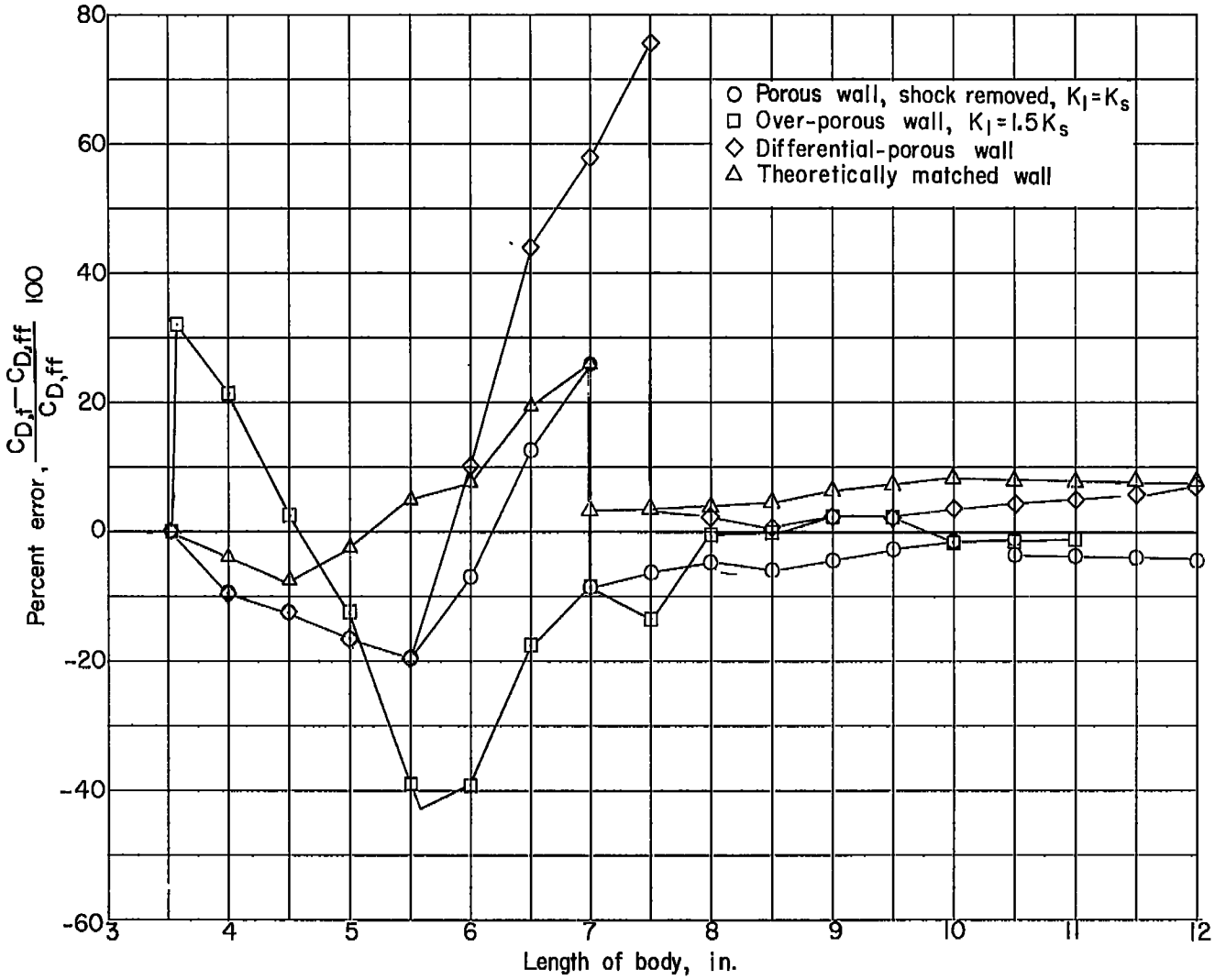

Figure 14.- Percentage error in drag of a cone-cylinder model restrained by various walls.

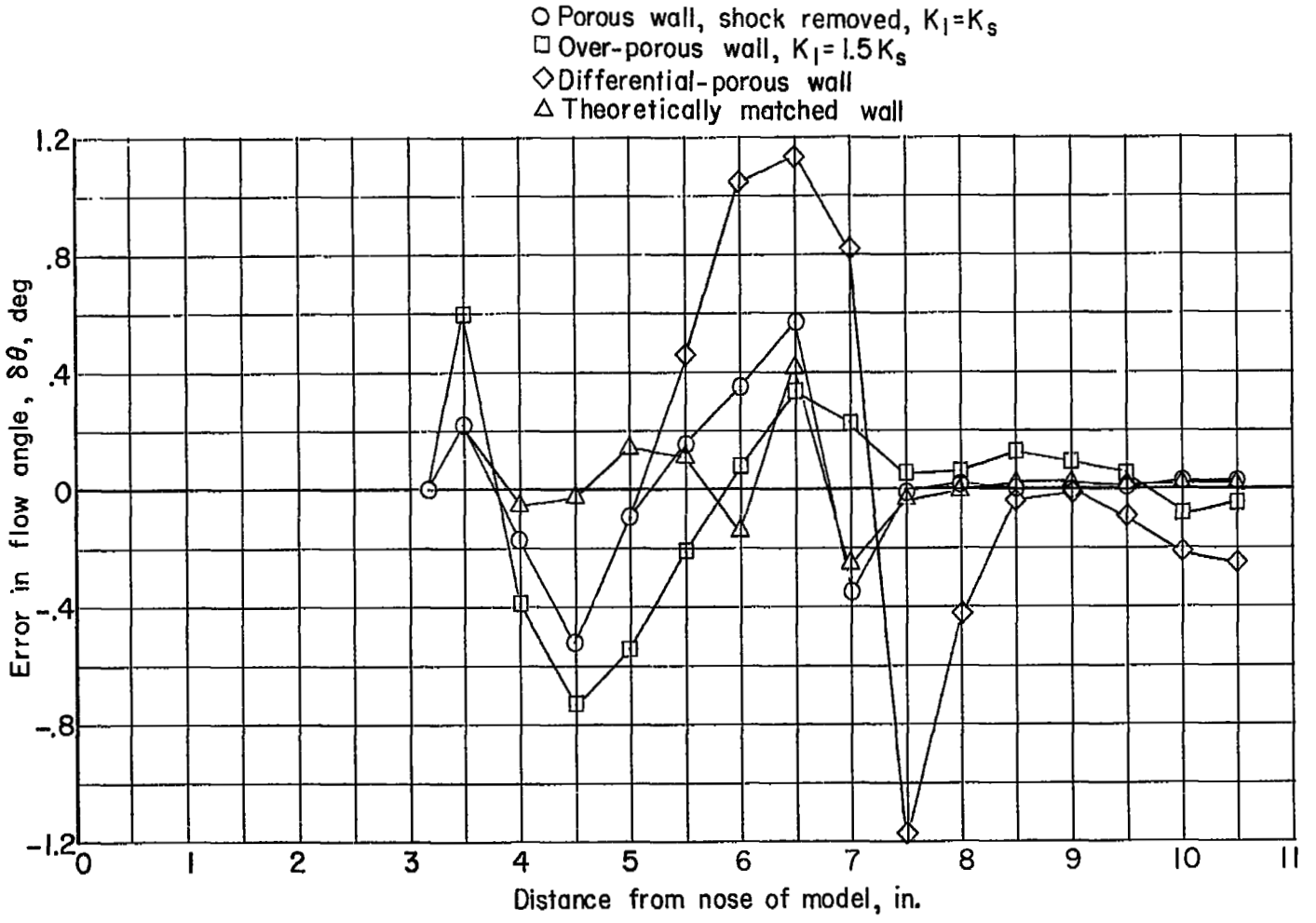

Figure 15.- Error in flow angle at 1-inch radius from a 0.94-inch-diameter conc-cylinder model with flow restricted by various walls. $M_\infty = 1.194$; blockage, 1.796 percent.